

Dynamics of 1,2-Hydrogen Migration in Carbenes and Ring Expansion in Cyclopropylcarbenes

Titus V. Albu, Benjamin J. Lynch, and Donald G. Truhlar*

Department of Chemistry and Supercomputer Institute, University of Minnesota,
Minneapolis, Minnesota 55455-0431

Alan C. Goren,[†] David A. Hrovat, and Weston Thatcher Borden

Department of Chemistry, Box 351700, University of Washington, Seattle, Washington 98195-1700

Robert A. Moss

Department of Chemistry and Chemical Biology, Rutgers, The State University of New Jersey,
New Brunswick, New Jersey 08903

Received: February 27, 2002

Variational transition state theory with multidimensional tunneling contributions has been used to calculate the rate constants, kinetic isotope effects, and activation energies for 1,2-shifts in methylchlorocarbene, benzylchlorocarbene, cyclopropylfluorocarbene, and cyclopropylchlorocarbene. Calculations have been performed for the rearrangements both in the gas phase and in various solvents. Including solvation effects reduces the calculated activation barrier for each of these reactions. The effects of quantum mechanical tunneling are computed to be significant for the 1,2-hydrogen migrations and to be bigger for hydrogen than for deuterium. Consequently, the deuterium kinetic isotope effects are predicted to be relatively large but to decrease with increasing temperature. In contrast, tunneling is not calculated to play a significant role in either of the halocyclopropylcarbene rearrangements, which both involve the 1,2-shift of a CH₂ group. Thus, heavy-atom tunneling is apparently not responsible for the fact that the calculated activation parameters are very different from experiment for cyclopropylfluorocarbene, with the experimental activation enthalpy much smaller than the calculated one and the experimental activation entropy much more negative than the computed value. Possible causes for the large differences between the calculated and measured activation parameters are discussed.

1. Introduction

With few exceptions,^{1,2} most singlet alkyl or alkylaryl carbenes undergo rapid intramolecular 1,2-hydrogen, alkyl, or aryl migrations to form alkenes^{3–5} or react by other fast intermolecular processes.^{6–11} The intramolecular rearrangements have been the focus of extensive investigations, both experimental^{3–5,9,11–59} and theoretical.^{52,53,60–70}

Carbenes are often produced by photolysis or thermolysis of diazirines. However, the extent to which free, electronically unexcited carbenes are actually involved in the 1,2-shifts that occur on photolysis of diazirine precursors remains the subject of ongoing research. It has been proposed that the product observed after such photolyses might in fact be formed, at least in part, in an excited electronic state of the diazirines^{31,41,48–51,63} or in a complex formed between the carbene and an olefin present in the system^{16,24} or between the carbene and the solvent.^{42,54} Concurrent rearrangement by more than one of these mechanisms has also been invoked.^{43,57}

The kinetic parameters computed for the rearrangements of the free carbenes are generally very different from those measured for the 1,2-shifts that occur when diazirine precursors

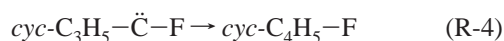
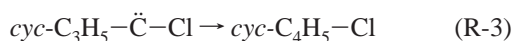
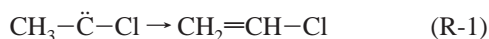
of the putative carbenes are photolyzed. The experimentally determined Arrhenius activation energy E_a and the phenomenological enthalpy of activation derived from it, which we call ΔH_{act} , are usually considerably smaller than the values computed by conventional transition state theory (TST), for which we reserve the symbols E_a^\ddagger and ΔH^\ddagger . In addition, the experimental value for the phenomenological entropy of activation, ΔS_{act} , is usually much more negative than the computed TST value, ΔS^\ddagger .

Factors that might account for these differences include the following: (i) limitations in accuracy of the electronic structure methods that have been applied; (ii) strong solvent effects that render the electronic structure calculations for the gas-phase reactions inapplicable to the experimental results, all of which have been obtained in solution; (iii) dynamical effects that necessitate the use of variational transition state theory in calculations on these reactions; (iv) a significant contribution of tunneling to the observed rates; and (v) rearrangements by pathways that do not involve free carbenes. This paper describes the results of a theoretical investigation of whether some or all of the first four of these factors are the cause of the differences between the computed and measured kinetic parameters.

We have performed calculations on four carbene rearrangements, involving 1,2-migrations. The reactions that we have studied are the following:

* Corresponding author. E-mail: truhlar@umn.edu.

[†] Permanent address: Department of Chemistry, Transylvania University, Lexington, KY 40508.



We chose these reactions because they have previously been studied both computationally and experimentally, and the computational and the experimental results disagree in the manner described above. For example, the rearrangement of methylchlorocarbene to vinyl chloride (reaction R-1) in *n*-heptane has been reported to have an E_a of 4.9 kcal/mol,²¹ whereas MP4/6-311G(d,p)//MP2/6-31G(d) calculations on this reaction in the gas phase give a zero-point-inclusive barrier height of 11.5 kcal/mol.⁶⁰

Similarly, for the rearrangement of benzylchlorocarbene to *Z*- and *E*- β -chlorostyrenes (reaction R-2), experimentally determined E_a values range from 4.5 to 4.8 kcal/mol in isooctane²⁴ (5.8 kcal/mol in isooctane when corrections for reaction with the solvent are included⁴²) down to 3.6 kcal/mol in chloroform⁴² and 3.2 kcal/mol in 1,1,2,2-tetrachloroethane^{46,54}. However, B3LYP/6-311G(d,p)//B3LYP/6-31G(d) calculations give classical barrier heights of 7.3 and 10.0 kcal/mol for formation of the *E*- and *Z*-product, respectively, in the gas phase.⁶⁹

Some time ago, Krogh-Jespersen, Moss, et al. pointed out the discrepancy between calculations and experiments regarding the activation parameters for reaction R-3.^{20,23} Krogh-Jespersen and co-workers calculated²⁰ (HF/6-311G(d)//HF/6-31G(d)) $\Delta H^\ddagger = 8.2$ kcal/mol and $\Delta S^\ddagger = -2.7$ cal mol⁻¹ K⁻¹, in comparison to the experimental values of, respectively, about 2–3 kcal/mol and about –20 to –24 cal mol⁻¹ K⁻¹.²³

In this paper, we report the results of direct dynamics calculations on these carbene rearrangements, both in the gas phase and in solution. These calculations include the contributions of quantum mechanical tunneling to the rate constants. In addition, for the rearrangement of methylchlorocarbene to vinyl chloride (reaction R-1) and of cyclopropylfluorocarbene to 1-fluorocyclobutene (reaction R-4), we have tested the convergence of the electronic structure theory calculations by recomputing the activation parameters with a wide variety of different methods.

We find that the agreement between the computed and the experimental kinetic parameters for the carbene rearrangements in R-1 and R-2 is improved when both solvation and tunneling effects are included in the calculations. However, the agreement is still not satisfactory. Solvation effects are also computed to reduce ΔH^\ddagger for the cyclopropylhalocarbene rearrangements in R-3 and R-4, but our calculations find little contribution from tunneling in either of these reactions. Consequently, even after investigation of possible contributions from (i) inaccuracies in the electronic structure theory calculations, (ii) solvation, (iii) dynamical effects, and (iv) tunneling, significant differences between the computed and the measured activation parameters for these rearrangements persist. These differences are especially striking for the 1,2-shift in cyclopropylfluorocarbene. Possible reasons for the persistence of this discrepancy are discussed.

2. Computational Methodology and Quantities Calculated

All the rearrangements in this paper were assumed to proceed on the ground-state singlet surface of the carbenes. The rate constants were calculated by using variational transition state theory with multidimensional tunneling contributions.^{71–77} The

canonical variational-transition-state theory (CVT) rate constant, k^{CVT} , was obtained by maximizing the generalized free energy of activation (at temperature T), ΔG_T^{GT} , as a function of the position, s , of the generalized transition state along the isoenergetic minimum energy path (MEP). The CVT free energy of activation is obtained as

$$\Delta G_T^{\text{CVT}} = \max_s \Delta G_T^{\text{GT}} \quad (1)$$

At the saddle point ($s = 0$) one obtains the conventional TST rate constant, k^{TST} , and the saddle point free energy of activation ΔG_T^\ddagger .

Quantum mechanical effects along the reaction coordinate were included in this study in the form of temperature-dependent transmission coefficients, κ . The transmission coefficients primarily account for the multidimensional tunneling (MT), and they were computed using the centrifugal-dominant, small-curvature, semiclassical, adiabatic, ground-state tunneling (called small-curvature tunneling or SCT) approximation.^{78,79} Rate constants including tunneling contributions were computed from the following expression:

$$k^{\text{CVT/SCT}}(T) = \kappa^{\text{SCT}} k^{\text{CVT}} = \kappa^{\text{SCT}} (k_B T/h) \exp(-\Delta G_T^{\text{CVT}}/RT) \quad (2)$$

where κ^{SCT} is the transmission coefficient, k_B is Boltzmann's constant, h is Planck's constant, and R is the gas constant.

We carried out the direct dynamics calculations by using the GAUSSRATE⁸⁰ computer program, which interfaces the POLYRATE⁸¹ and *Gaussian*⁸² programs. The MEP in isoenergetic coordinates was calculated by the Page-McIver method.⁸³ The coordinates were scaled to a reduced mass μ of 1 amu for reactions R-1 and R-2 and to a reduced mass μ of 12 amu for reactions R-3 and R-4. (All physical observables are independent of μ , which only affects the scale of the coordinate system, the values of s assigned to stationary points, and the sizes of steps along s .) For reactions R-1, R-3, and R-4, we used a step size of 0.005 a_0 between gradient calculations, and a Hessian was calculated every 0.05 a_0 along the MEP. For reaction R-2 we used a gradient step size of 0.010 a_0 and a Hessian step size of 0.09 a_0 . Calculations were carried out far enough along the reaction path to converge the tunneling calculations.

The vibrational frequencies along the reaction path were evaluated using a set of redundant internal coordinates⁸⁴ that consists of six stretches, ten nondegenerate bends, and three torsions for reaction R-1, consists of seventeen stretches, twenty-eight nondegenerate bends, and twenty-one torsions for reaction R-2, and consists of eleven stretches, twenty-three nondegenerate bends, and three torsions for reactions R-3 and R-4. These choices of the redundant internal coordinates that were used in generalized, normal-mode, vibrational analyses, yielded in each case a reaction-path Hamiltonian with all frequencies real along the portion of the MEP that was investigated. The vibrational partition functions were calculated assuming the harmonic approximation for all vibrations.

The levels of electronic structure theory used for the gas-phase dynamics calculations were MP2(full)/6-31G(d),⁸⁵ MPW1K/6-31+G(d,p),⁸⁶ and mPW1PW91/6-31+G(d,p)⁸⁷ for reaction R-1, MPW1K/6-31+G(d,p) and mPW1PW91/6-31+G(d,p) for reaction R-2, and mPW1PW91/6-31+G(d,p) for reactions R-3 and R-4. Henceforth, we use the shorthand notation HDFT (hybrid density functional theory) to denote the results from the mPW1PW91/6-31+G(d,p) hybrid of Hartree–Fock and density functional theory.

For reactions R-1 and R-4 additional electronic structure calculations were performed. They included B3LYP (which is another version of HDFT),^{88–90} CBS-Q,⁹¹ MC-QCISD//ML,^{92,93} and MCG3//ML^{93–95} for reaction R-1. MC-QCISD//ML^{92,93} and MCG3//ML^{93–95} involve geometry optimization with multi-coefficient correlation methods that, in principle, provide an extrapolation to complete configuration interaction.^{93,96} (Note that //ML denotes multilevel optimizations as discussed elsewhere.⁹³) B3LYP, CBS-Q, CBS-APNO,⁹¹ MC-QCISD, MCG3, (10/10)CASSCF,⁹⁷ and (10/10)CASPT2⁹⁸ calculations were carried for reaction R-4. The (10/10) active space for the latter calculations consisted of the bonding and antibonding orbitals for all the C–C bonds, plus the σ and π nonbonding molecular orbitals of the carbenic center. Single-point CASPT2 calculations were also carried out at the (10/10)CASSCF/6-31G(d) stationary points with the cc-pVTZ⁹⁹ basis set, which includes two sets of d and one set of f polarization functions on the heavy atoms and two p and one d set of polarization functions on the hydrogen atoms.

The MP2, MPW1K, mPW1PW91, B3LYP, and CBS calculations were carried out using the Gaussian 98 suite of programs,⁸² the CASSCF and CASPT2 calculations were performed with MOLCAS,¹⁰⁰ and the MC-QCISD and MCG3 calculations were carried out with MULTILEVEL¹⁰¹ using version 2m⁹² coefficients in both cases. For the calculations on the solution-phase reactions, Gaussian 98⁸² was combined with the MN-GSM solvation module.¹⁰²

Solvation effects were included using the generalized Born (GB) approximation^{103–114} and the SM5.42R solvation model.^{114–117} For the GB calculations we used Class II charges calculated by Löwdin population analysis¹¹⁸ while for the SM5.42R we used Class IV charges calculated by CM2.¹¹⁹ In the GB calculations, the potential of the mean force in solution was determined as the sum of the solute's potential energy and the electrostatic energy of solvation. The SM5.42R calculations also included nonbulk (or specific) first solvation-shell effects, in particular, cavitation, dispersion, and solvent structural effects.¹¹⁴ All solvation parameters (e.g., atomic radii and atomic surface tensions) were approximated as being independent of T , and standard values of these parameters¹¹⁷ were used.

For the GB calculations, only the bulk electrostatic component of solvation was included, and dielectric descreening was treated as in SM5.42R.^{112,115,120} The dynamics in solution were simulated using the equilibrium solvation path (ESP) approach,^{121,122} in which stationary point geometries and reaction path are optimized in the liquid phase. These GB/mPW1PW91/6-31+G(d,p) calculations are denoted GB/HDFT. Additional dynamics calculations were carried out using the separable equilibrium solvation (SES) approximation^{121,122} in which solvation free energies are computed using gas-phase solute structures and reaction paths. These calculations could be labeled as mPW1PW91/6-31+G(d,p) + GB/mPW1PW91/6-31+G(d,p)//mPW1PW91/6-31+G(d,p), but we prefer to use the more convenient, shorthand notation HDFT+GB.

SM5.42R calculations should provide a better model of the solvation effects than GB calculations. The present SM5.42R calculations are carried out at the HF/6-31G(d) level of theory. For the SM5.42R model, the dynamics in solution were carried out using the SES approximation. These calculations could be labeled as mPW1PW91/6-31+G(d,p) + SM5.42R/HF/6-31G(d)//mPW1PW91/6-31+G(d,p), but we use the notation DFT+SM.

For the dynamics calculations that use the SES approximation, the calculated free energies of solvation are added to the

mPW1PW91/6-31+G(d,p) potential energy along the gas-phase reaction path. This is accomplished by using an interpolated single-point energies (ISPE) algorithm.¹²³ Specifically, we use ISPE-2,¹²³ where the interpolation is based on single-point solution calculations at the reactant, the product, the saddle point, and two additional points, located on a $0.01a_0$ grid, at geometries 1/3 down in energy from the saddle point toward the reactant and toward the product, respectively. (ISPE calculations require, for unimolecular reactions with one product, an estimate of the value of s for the reactant and the product. We approximated these values as three times the s value of the additional points used in the ISPE-2 calculation.) For SES calculations we define the conventional transition state in the liquid to be located at the gas-phase saddle point.

For interpretive purposes we also computed dipole moments of all reactants, transition states, and products in the standard way from mPW1PW91/6-31+G(d,p) wave functions and also from the CM2/HF/6-31G(d)¹¹⁹ partial atomic charges that are used in the solvation model.

The results of our calculations are presented in a series of tables in the next section. In these tables $k^{V/T}$ is a shorthand notation for $k^{CVT/SCT}$, ΔE is the classical energy of reaction, V^\ddagger is the classical (i.e., zero-point-exclusive) barrier height, and ΔH_0^\ddagger is the zero-point-inclusive barrier height. The latter is calculated as

$$\Delta H_0^\ddagger = V^\ddagger + \sum_{m=1}^{N_{\text{vib}}^\ddagger} \frac{\hbar\omega_m^\ddagger}{2} - \sum_{m=1}^{N_{\text{vib}}^R} \frac{\hbar\omega_m^R}{2} \quad (3)$$

where ω_m^\ddagger and ω_m^R are the frequency of the normal mode m for the saddle point and reactant, respectively, $N_{\text{vib}}^\ddagger = 3N_{\text{atoms}} - 7$, $N_{\text{vib}}^R = 3N_{\text{atoms}} - 6$, and N_{atoms} is the number of atoms in the system.

Theoretical values of phenomenological free energies of activation ΔG_T^{TST} and $\Delta G_T^{V/T}$ at 298 K have been determined by fitting k^{TST} and $k^{V/T}$ to:

$$k^{\text{TST}}(298) = (k_B T/h) \exp(-\Delta G_{298}^\ddagger/RT) \quad (4)$$

$$k^{V/T}(298) = (k_B T/h) \exp(-\Delta G_{298}^{V/T}/RT) \quad (5)$$

which yields

$$\Delta H_{298}^\ddagger = R T_1 T_2 / (T_2 - T_1) \ln[k^{\text{TST}}(T_2) T_1 / k^{\text{TST}}(T_1) T_2] \quad (6)$$

$$\Delta S_{298}^\ddagger = (\Delta H_{298}^\ddagger - \Delta G_{298}^\ddagger) / T \quad (7)$$

$$\Delta H_{298}^{V/T} = R T_1 T_2 / (T_2 - T_1) \ln[k^{V/T}(T_2) T_1 / k^{V/T}(T_1) T_2] \quad (8)$$

$$\Delta S_{298}^{V/T} = (\Delta H_{298}^{V/T} - \Delta G_{298}^{V/T}) / T \quad (9)$$

where $T = 298$ K, $T_1 = 293$ K, and $T_2 = 303$ K. It should be pointed out that ΔH_{298}^\ddagger and ΔS_{298}^\ddagger , obtained according to eqs 6 and 7, have exactly the same values as ΔH_{298}^\ddagger and ΔS_{298}^\ddagger that are given for the gas-phase calculations by the thermochemical analyses in the electronic structure software. This agreement is an indication that the two-temperature fit that we used provides correct results.

Theoretical Arrhenius parameters A and E_a at 298 K have been determined by fitting k^{TST} and $k^{V/T}$ to

$$k = A \exp(-E_a/RT) \quad (10)$$

which yields

$$E_a^\ddagger = R T_1 T_2 / (T_2 - T_1) \ln[k^{\text{TST}}(T_2) / k^{\text{TST}}(T_1)] \quad (11)$$

$$A^\ddagger = k^{\text{TST}}(298) \exp(E_a^\ddagger / RT) \quad (12)$$

$$E_a^{V/T} = R T_1 T_2 / (T_2 - T_1) \ln[k^{V/T}(T_2) / k^{V/T}(T_1)] \quad (13)$$

$$A^{V/T} = k^{V/T}(298) \exp(E_a^{V/T} / RT) \quad (14)$$

where $T = 298$ K, $T_1 = 293$ K, and $T_2 = 303$ K.

For the reactions investigated here, at all levels of theory, the variational effect was not significant. The calculated values of k^{TST} and k^{CVT} were within 2% of each other for the gas-phase and equilibrium solvation path (ESP) calculations and within 5% for the separable equilibrium solvation (SES) calculations. Therefore, we chose to report only k^{CVT} .

A more accurate treatment of tunneling would be to employ canonically optimized multidimensional tunneling,¹²⁴ which involves choosing the larger of the SCT and large-curvature tunneling (LCT)^{125,126} transmission coefficients at each temperature. We found that for reactions R-1 and R-2 the SCT are greater than the LCT transmission coefficients, while for reactions R-3 and R-4 the two types of transmission coefficients are practically equivalent. Consequently, only the results of the SCT calculations are included in the tables.

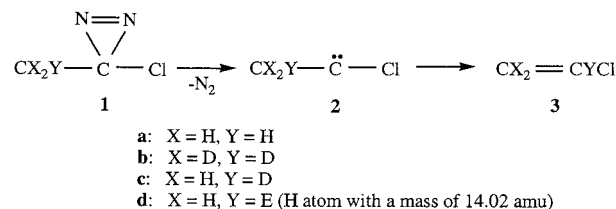
All kinetic isotope effects (KIEs) are expressed, as usual, with the lighter atom in the numerator. Thus, the hydrogen/deuterium KIE is k_H/k_D .

3. Results and Discussion

3.1. Temperature Dependence of the Activation Parameters. In the process of studying possible reasons for the discrepancies between theory and experiment, we examined the temperature dependence of the computed Arrhenius parameters. A selection of results is shown in Table 1. Especially for the 1,2-hydrogen shift in methylchlorocarbene (R-1) and in benzylchlorocarbene (R-2), this table shows a strong dependence of the CVT/SCT Arrhenius activation energies on temperature, which is due almost entirely to tunneling. Thus, in the subsequent sections we are careful to compare theory to experiment over the same temperature intervals as were studied experimentally.

3.2. 1,2-Hydrogen Migration in Methylchlorocarbene. First we reinvestigated the KIE and tunneling contributions to the 1,2-H migration in methylchlorocarbene (**2** in Scheme 1). Previous calculations of these KIEs and tunneling contributions have been published by Storer and Houk.⁶²

SCHEME 1



Thermal^{127,128} and photochemical^{129–132} decomposition of 3-chloro-3-methyldiazirine (**1**) to form vinyl chloride (**3**) has been studied experimentally in the gas phase. However, to our knowledge, there are no reports of the gas-phase kinetic parameters for the second-step in the formation of **3**, 1,2-hydrogen migration in methylchlorocarbene (**2**). The only experimental kinetic parameters that are available for this step are for the reaction in solution. To try to sort out possible solvent effects, we carried out dynamics calculations on the rearrangement of **2** to **3** (R-1) in the gas phase and in two different solvents, *n*-heptane and 1,2-dichloroethane.

In an experimental study, Dix et al.³⁴ reported a low activation enthalpy and a very negative activation entropy for the 1,2-H migration in **2**. These results were interpreted as resulting from quantum mechanical tunneling at low temperatures. However, reactions that involve large amounts of tunneling usually have large k_H/k_D KIEs that decrease with increasing temperature (as tunneling becomes less important) whereas the KIE, $k_H/k_D = k(\mathbf{2a} \rightarrow \mathbf{3a})/k(\mathbf{2b} \rightarrow \mathbf{3b})$, measured by Dix et al.³⁴ was found not only to be very small but also to increase with temperature, from 0.9 at 248 K to 1.8 at 343 K. Similar results were reported for the 1,2-H migration in methylbromocarbene.⁴⁰

Although surprising, these experimental results were, nevertheless, supported by the results of an MP2(full)/6-31G(d) theoretical study by Storer and Houk.⁶² Their calculations found that hydrogen atom tunneling reduces the activation energy for the 1,2-shift in methylchlorocarbene by 3.2 kcal/mol at 298 K, although their calculated activation energy is still 2.8 kcal/mol higher than the experimental value of 4.9 kcal/mol.²¹ More importantly, the deuterium KIE was calculated to decrease when tunneling contributions were added to the computed rate constants. Not only was the tunneling contribution computed to be greater for deuterium than for hydrogen, but also the results of calculations in which the mass of the transferred atom was artificially increased to 14.02 amu (as in **2d** \rightarrow **3d**) suggested that heavy-atom tunneling was a strong possibility in such carbene rearrangements.

There are several reports in the literature of enzymatic¹³³ and nonenzymatic^{134–137} reactions in which the tunneling contributions have been calculated to be larger for deuterium than for

TABLE 1: Calculated Activation Energies E_a^{CVT} and $E_a^{\text{CVT/SCT}}$ (kcal/mol) at Different Temperatures for the 1,2-Protium Migrations in Methylchlorocarbene (**2a** \rightarrow **3a**) and Benzylchlorocarbene (**5a** \rightarrow **6a** + **7a**) and for the 1,2-Methylene Migrations in Cyclopropylchlorocarbene (**9a** \rightarrow **10a**) and Cyclopropylfluorocarbene (**12** \rightarrow **13**)^{a,b}

<i>T</i> (K)	2a \rightarrow 3a		5a \rightarrow 6a		5a \rightarrow 7a		9a \rightarrow 10a		12 \rightarrow 13	
	CVT	CVT/SCT	CVT	CVT/SCT	CVT	CVT/SCT	CVT	CVT/SCT	CVT	CVT/SCT
175	10.25	1.97	7.79	2.11	5.33	2.75	9.71	8.80	12.41	11.12
200	10.26	3.25	7.80	4.21	5.36	3.42	9.73	9.02	12.43	11.49
225	10.27	4.75	7.82	5.59	5.39	3.86	9.75	9.16	12.44	11.69
250	10.28	6.06	7.84	6.24	5.41	4.15	9.77	9.27	12.46	11.83
298	10.30	7.59	7.88	6.78	5.45	4.50	9.80	9.40	12.49	12.00
365	10.33	8.55	7.92	7.11	5.50	4.78	9.84	9.53	12.52	12.14

^a Determined using CVT and CVT/SCT rate constants obtained from HDFT+GB(isooctane) calculations (HDFT \equiv mPW1PW91/6-31+G(d,p) and GB \equiv GB/mPW1PW91/6-31+G(d,p)//mPW1PW91/6-31+G(d,p)). ^b The CVT/SCT calculations include tunneling contributions; the CVT calculations do not.

TABLE 2: Calculated and Experimental Rate Constants (10^5 s^{-1}) and Deuterium Kinetic Isotope Effect, KIE, for the 1,2-Hydrogen Rearrangement of Methylchlorocarbene ($2 \rightarrow 3$)

T (K)	theory ^a		theory ^b		experiment	
	$k(2a \rightarrow 3a)$	KIE	$k(2a \rightarrow 3a)$	KIE	$k(2a \rightarrow 3a)$	KIE
295	gas phase		<i>n</i> -heptane		<i>n</i> -heptane ^c	
	0.99	7.6	4.0	6.4	13.5	
203	gas phase		<i>n</i> -heptane		<i>n</i> -heptane ^d	
	0.012	130	0.050	69	6.1	
238	0.059	26	0.26	18	6.6	
273	0.34	11	1.5	8.6	8.0	
298	1.1	7.3	4.6	6.2	10.5	
310	1.9	6.4	7.6	5.5	17.5	
333	5.1	5.1	19	4.6	30.4	
353	11	4.4	38	4.0	46.3	
248	gas phase		1,2-dichloroethane		1,2-dichloroethane ^e	
	0.098	19	2.7	11	8.4	0.9
273	0.34	11	8.5	7.6	9.2	1.1
294	0.94	7.7	21	5.9	12.1	1.4
313	2.2	6.1	43	5.0	14.9	1.6
343	7.6	4.7	120	4.1	30.8	1.8

^a CVT/SCT results at the mPW1PW91/6-31+G(d,p) level of theory.

^b CVT/SCT results at the GB/mPW1PW91/6-31+G(d,p) level of theory.

^c Ref 21. ^d Ref 40. ^e Ref 34.

hydrogen. In these reports, however, the barriers have been low and broad; so the tunneling contributions have been small compared to overbarrier processes. In such cases, the smaller effective barrier for H transfer than for D transfer results in a normal KIE for passage over the barrier; but it also makes tunneling through the barrier more important for D than for H.

In the rearrangement of **2** to **3**, where the barrier height is appreciable, the usual finding of larger tunneling for the lighter isotope would be anticipated. In fact, we were unable to reproduce the results of Storer and Houk's calculations. The results of our calculations, which are presented in Table 2, show a large normal KIE that decreases with increasing temperature, as more of the molecules cross the barrier, rather than tunnel

through it. The difference between the results of our calculations and those of Storer and Houk has been traced to an error in their calculations.¹³⁸

Gas-phase calculations on chloromethylchlorocarbene by Keating et al.⁶⁵ are in qualitative agreement with the present gas-phase calculations, although they considered only the all-protium case and used a less reliable tunneling approximation than ours. They found that tunneling lowers the activation energy at 298 K from 8.5 to 5.9 kcal/mol, as compared to a lowering from 11.3 to 8.1 kcal/mol in the present mPW1PW91/6-31+G-(d,p) calculation on methylchlorocarbene.

As shown in Table 3, in our calculations on the rearrangement of **2** to **3** in the liquid-phase, using the GB model, the classical, gas-phase barrier height (V^\ddagger) is reduced by 1.0 kcal/mol in *n*-heptane (dielectric constant $\epsilon = 1.911$) and by 2.0 kcal/mol in 1,2-dichloroethane ($\epsilon = 10.125$). Similar differences are seen in the Arrhenius activation energies (E_a^\ddagger), computed by conventional TST. Using the SM model, solvation effects are computed to lower the classical barrier height a little more, by 1.9 and 3.5 kcal/mol in *n*-heptane and 1,2-dichloroethane, respectively.

The reason that the solvent stabilizes the transition structure more than the reactant is that transfer of electron density to the carbenic carbon occurs during the course of the hydrogen migration. In particular, in the gas phase, the CM2/HF/6-31G-(d) charge on the carbenic carbon is initially +0.005 and changes to -0.19 at the saddle point and to -0.08 at the product. In *n*-heptane, the corresponding values are 0.001, -0.21, and -0.08, and in 1,2-dichloroethane, they are -0.002, -0.22, and -0.10, respectively. The dipole moment of the transition structure is computed to be well over 1 D larger than that of methylchlorocarbene, as shown in Table 4.

Table 4 shows the dipole moments calculated from CM2 partial atomic charges, which are the charges used in our solvation model. These charges underestimate the dipole moments of the carbene reactants calculated from the electron density by an average of 0.9 D. This may be a general systematic

TABLE 3: Energetic and Kinetic Parameters for the Methylchlorocarbene Rearrangement^a

reaction	ΔE	V^\ddagger	ΔH_0^\ddagger	ΔH_{298}^\ddagger	ΔS_{298}^\ddagger	E_a^\ddagger	A^\ddagger	$\Delta H_{298}^{V/T}$	$\Delta S_{298}^{V/T}$	$E_a^{V/T}$	$A^{V/T}$
MP2/6-31G(d)											
2a \rightarrow 3a	-64.3	13.6	12.0	11.6	-3.1	12.2	3.5(12) ^b	7.7	-11.7	8.3	4.8(10)
2b \rightarrow 3b	-64.3	13.6	12.5	12.1	-3.5	12.7	2.9(12)	10.4	-6.9	11.0	5.3(11)
2c \rightarrow 3c	-64.3	13.6	12.5	12.0	-3.5	12.6	2.9(12)	10.2	-7.2	10.8	4.6(11)
2d \rightarrow 3d	-64.3	13.6	13.0	12.6	-4.3	13.1	1.9(12)	12.1	-5.2	12.7	1.2(12)
MPW1K/6-31+G(d,p)											
2a \rightarrow 3a	-58.5	13.5	12.0	11.6	-3.1	12.2	3.5(12)	8.1	-10.6	8.7	8.2(10)
2b \rightarrow 3b	-58.5	13.5	12.5	12.1	-3.5	12.6	2.9(12)	10.6	-6.5	11.2	6.6(11)
HDFT ^c											
2a \rightarrow 3a	-58.0	12.6	11.1	10.7	-3.4	11.3	3.0(12)	7.5	-10.1	8.1	1.0(11)
2b \rightarrow 3b	-58.0	12.6	11.6	11.2	-3.8	11.8	2.5(12)	9.8	-6.5	10.4	6.3(11)
GB/HDFT ^d (<i>n</i> -heptane)											
2a \rightarrow 3a	-57.7	11.6	10.1	9.7	-3.4	10.3	3.1(12)	7.1	-8.9	7.7	1.9(11)
2b \rightarrow 3b	-57.7	11.6	10.6	10.2	-3.8	10.8	2.5(12)	9.0	-6.2	9.6	7.6(11)
GB/HDFT ^d (1,2-dichloroethane)											
2a \rightarrow 3a	-57.4	10.6	9.0	8.6	-3.3	9.2	3.2(12)	6.4	-7.9	7.0	3.2(11)
2b \rightarrow 3b	-57.4	10.6	9.5	9.1	-3.7	9.7	2.6(12)	8.1	-5.7	8.7	9.5(11)
HDFT+SM ^e (<i>n</i> -heptane)											
2a \rightarrow 3a	-58.3	10.7	9.1	8.7	-3.4	9.3	3.0(12)	6.4	-8.3	6.9	2.6(11)
2b \rightarrow 3b	-58.3	10.7	9.6	9.2	-3.8	9.8	2.5(12)	8.1	-5.9	8.7	8.5(11)
HDFT+SM ^e (1,2-dichloroethane)											
2a \rightarrow 3a	-58.4	9.1	7.6	7.2	-3.4	7.8	3.0(12)	5.4	-7.1	6.0	4.7(11)
2b \rightarrow 3b	-58.4	9.1	8.1	8.7	-3.8	8.3	2.5(12)	6.8	-5.5	7.4	1.1(12)

^a ΔE , V^\ddagger , ΔH_0^\ddagger , ΔH_{298}^\ddagger , $\Delta H_{298}^{V/T}$, E_a^\ddagger , and $E_a^{V/T}$ in kcal/mol; ΔS_{298}^\ddagger and $\Delta S_{298}^{V/T}$ in cal mol⁻¹ K⁻¹; A^\ddagger and $A^{V/T}$ in s⁻¹. ^b 3.5(12) \equiv 3.5×10^{12} . ^c HDFT \equiv mPW1PW91/6-31+G(d,p). ^d GB/HDFT \equiv GB/mPW1PW91/6-31+G(d,p). ^e SM \equiv SM5.42R/HF/6-31G(d)/mPW1PW91/6-31+G(d,p).

TABLE 4: Dipole Moments (Debye) for Stationary Points in the 1,2-Proton Migration in Methylchlorocarbene and Benzylchlorocarbene and in the 1,2-Methylene Migration in Cyclopropylchlorocarbene and Cyclopropylfluorocarbene^a

molecule	gas phase ^b	gas phase ^c	isooctane ^c
methylchlorocarbene	2.42	1.42	1.56
transition state	3.38	2.96	3.27
vinyl chloride	1.56	1.34	1.49
benzylchlorocarbene	2.13	1.24	1.32
(<i>Z</i>)-transition state	4.14	3.12	3.49
(<i>Z</i>)- β -chlorostyrene	1.50	1.40	1.60
benzylchlorocarbene	2.13	1.24	1.32
(<i>E</i>)-transition state	4.05	3.51	3.80
(<i>E</i>)- β -chlorostyrene	1.89	1.75	1.91
cyclopropylchlorocarbene	3.45	2.71	3.02
transition state	4.37	4.10	4.55
1-chlorocyclobutene	1.87	1.66	1.85
cyclopropylfluorocarbene	3.35	2.44	2.72
transition state	4.11	3.88	4.32
1-fluorocyclobutene	1.75	1.79	1.99

^a All geometries are gas-phase geometries optimized by mPW1PW91/6-31+G(d,p). ^b mPW1PW91/6-31+G(d,p) dipole moments calculated in the standard way from the wave function. ^c HF/6-31G(d)/CM2 dipole moments.

error in using nuclear-centered partial charges based on population analysis for carbenic systems. The partial charge model also underestimates the dipole moments for transition states but in these cases by only about 0.5 D. The partial charge model works quite well for products.

The fact that solvation selectively stabilizes the transition structure was also noted in a previous computational study⁶⁴ of the 1,2-H migration in methylphenylcarbene. The value of ΔH_{298}^\ddagger was computed to decrease by 0.3 kcal/mol in *n*-heptane and by 1.0 kcal/mol in the more polar acetonitrile, compared to the gas phase. Since experimentally, the rate of the 1,2-H shift reaction in singlet methylphenylcarbene was found to increase by greater than 30-fold in acetonitrile compared to *n*-heptane (which corresponds to a decrease of about 2 kcal/mol in the Arrhenius activation energy), those calculations⁶⁴ appear to underestimate the effect of solvent polarity on the rate.

The acceleration with increased solvent polarity was attributed by Platz and co-workers to charge development in the transition state.²⁶ In particular, on the basis of substituent effects on the rate, Platz and co-workers inferred that little charge is developed at the carbenic carbon and that positive charge is developed at the carbon from which hydrogen migration occurs. Hence, they concluded that negative charge develops on the migrating hydrogen in the transition state (in keeping with the traditional view that the migrating H has some hydridic character) or that positive charge is decreased for the rearrangements of methylphenylcarbene and dimethylcarbene.^{26,27,52} For example, Ford et al.⁵² used Mulliken charge analysis to calculate that the charge on the migrating H in gas-phase dimethylcarbene decreases from +0.25 at the reactant to +0.10 at the transition state. The latter value is in excellent agreement with the value of +0.11 calculated earlier for the migrating hydrogen at the transition state in the rearrangement of methylphenylcarbene.⁶⁴

The calculated charges in the methylchlorocarbene (**2**) and the transition state of reaction R-1 are given in Figure 1, which shows a partial atomic charge on the migrating H of +0.23 to +0.25 in the transition state, compared to +0.14 to +0.15 in **2**. We also carried out a calculation on the rearrangement of dimethylcarbene at the same level of theory (CM2/HF/6-31G-

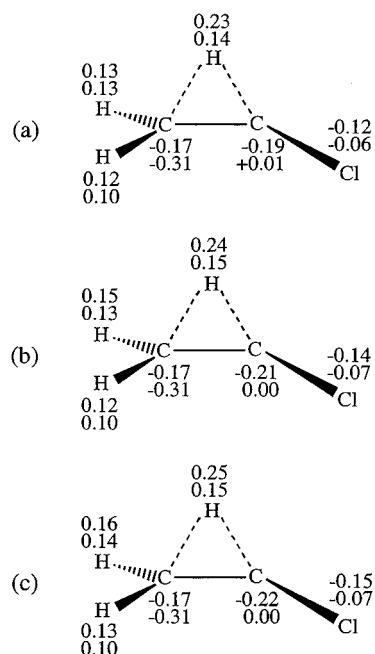


Figure 1. CM2 partial atomic charges on the transition state (upper entry) and the reactant (lower entry) for reaction R-1 as calculated by HF/6-31G(d) at mPW1PW91/6-31+G(d,p) gas-phase geometries: (a) gas phase, (b) in *n*-heptane, (c) in 1,2-dichloroethane.

(d)/mPW1PW91/6-31+G(d,p)); and we again found positive charge development on the migrating H in the transition structure. Its size was computed to be +0.22 in the gas phase and +0.24 in 1,2-dichloroethane, compared to +0.13 and +0.14, respectively, in the reactant, i.e., the charge on the migrating H increases by 0.09 to 0.10 in proceeding to the transition state. If we repeat our gas-phase calculation with Mulliken analysis, we find that charge on the migrating H at the reactant is +0.19 (instead of CM2 value of +0.13), and the charge at the transition state is +0.20 (instead of the CM2 value of +0.22).

For the rearrangement of **2**, the results in Figure 1 show that, on going from the reactant to the transition state, transfer of electrons to the carbenic carbon is greater than the transfer of electrons from the migrating hydrogen. The rest of the negative charge that is transferred to the carbenic carbon comes primarily from the carbon from which the hydrogen migrates, so that the latter carbon becomes less negative in the transition state for rearrangement of **2**. From the accelerating effect of a methyl group at this carbon, Platz and co-workers also deduced that electron density is lost by the carbon from which hydrogen migrates in the rearrangements of methylphenylcarbene and dimethylcarbene.^{26,27} Our calculations on the rearrangement of dimethylcarbene in 1,2-dichloroethane find a charge at this carbon of -0.19 in the transition structure, compared to -0.29 in the reactant. Ford et al.⁵² calculated -0.53 and -0.87, respectively, for these two partial charges by Mulliken analysis.

Further analysis of the charges may be unwarranted in light of the difficulty mentioned above in using nuclear-centered partial atomic charges based on population analysis to describe the present systems. It is important to emphasize, though, that the sign and the size of the charge on hydrogen depend on both the wave function and the method used for the population analysis. Additional discussion of partial charges to illustrate this point is provided in Supporting Information.

Table 3 shows that, when tunneling contributions are included in the CVT/SCT rate constants for the rearrangement of **2**, the effect of solvation on $E_a^{V/T}$ is smaller than the effect on E_a^\ddagger . Consequently, solvation makes the effect of tunneling on

TABLE 5: Rate Constants (s^{-1}), Calculated without (k^{CVT}) and with ($k^{V/T}$) Tunneling Contributions, SCT Transmission Coefficients, and the Imaginary Frequency (cm^{-1}) at the Saddle Point for the 1,2-Hydrogen Rearrangement of Methylchlorocarbene at 298 K

compound	k^{CVT}	$k^{V/T}$	κ	ω^\ddagger
MP2/6-31G(d)				
2a \rightarrow 3a	4.1(3) ^a	4.2(4)	10.3	1271 <i>i</i>
2b \rightarrow 3b	1.4(3)	4.4(3)	3.1	954 <i>i</i>
2c \rightarrow 3c	1.6(3)	5.4(3)	3.4	979 <i>i</i>
2d \rightarrow 3d	4.4(2)	6.3(4)	1.4	592 <i>i</i>
MPW1K/6-31+G(d,p)				
2a \rightarrow 3a	4.2(3)	3.3(4)	7.9	1229 <i>i</i>
2b \rightarrow 3b	1.5(3)	4.3(3)	2.8	924 <i>i</i>
HDFT ^b				
2a \rightarrow 3a	1.7(4)	1.1(5)	6.8	1206 <i>i</i>
2b \rightarrow 3b	5.9(3)	1.6(4)	2.6	907 <i>i</i>
GB/HDFT ^c (<i>n</i> -heptane)				
2a \rightarrow 3a	8.6(4)	4.6(5)	5.3	1155 <i>i</i>
2b \rightarrow 3b	3.1(4)	7.4(4)	2.4	869 <i>i</i>
GB/HDFT ^c (1,2-dichloroethane)				
2a \rightarrow 3a	5.5(5)	2.4(6)	4.4	1092 <i>i</i>
2b \rightarrow 3b	2.0(5)	4.2(5)	2.1	821 <i>i</i>
HDFT+SM ^d (<i>n</i> -heptane)				
2a \rightarrow 3a	4.4(5)	2.1(6)	4.7	
2b \rightarrow 3b	1.6(5)	3.5(5)	2.2	
HDFT+SM ^d (1,2-dichloroethane)				
2a \rightarrow 3a	5.4(6)	1.9(7)	3.5	
2b \rightarrow 3b	1.9(6)	3.7(6)	1.9	

^a 4.1(3) $\equiv 4.1 \times 10^3$. ^b HDFT \equiv mPW1PW91/6-31+G(d,p). ^c GB/HDFT \equiv GB/mPW1PW91/6-31+G(d,p). ^d SM \equiv SM5.42R/HF/6-31G(d)//mPW1PW91/6-31+G(d,p).

lowering the Arrhenius activation energy (i.e., the difference between E_a^\ddagger and $E_a^{V/T}$) smaller in solution than in the gas phase.

TABLE 6: Experimentally and Computationally Determined Arrhenius Activation Energies, Preexponential Factors, and Rate Constants at 298 K for 1,2-Migrations^a

reaction	E_a	$\log A$	T	k_{298}	solvent	reference ^b
2a \rightarrow 3a	4.9	9.7	285–334	0.01	<i>n</i> -heptane	21
	7.1	11.5	285–334	0.02	<i>n</i> -heptane	theory
	6.9	11.4	293–303	0.02	<i>n</i> -heptane	theory
5a \rightarrow 6a + 7a	6.4	12.2	283–385	0.3	tetramethylethylene	13
	4.5	11.1	273–304	0.6	isooctane	24
	4.8	11.3	269–307	0.6	isooctane	24
	5.8 ^c	11.9	193–333	0.4	isooctane	41
	3.0	12.1	193–333	79	isooctane	theory
	3.3	12.3	293–303	79	isooctane	theory
	3.6	10.4	218–333	0.6	chloroform	41
	2.8	12.3	218–333	167	chloroform	theory
	2.9	12.4	293–303	167	chloroform	theory
	3.3	10.1	202–276	0.5	1,1,2,2-tetrachloroethane	45
3.2	10.0	202–276	0.4	1,1,2,2-tetrachloroethane	53	
5b \rightarrow 6b + 7b	6.7 ^c	12.0	193–333	0.1	isooctane	41
	3.9	12.3	193–333	25	isooctane	theory
	4.1	12.4	293–303	25	isooctane	theory
	4.1	10.3	218–333	0.2	chloroform	41
	3.6	12.4	218–333	54	chloroform	theory
	3.7	12.4	293–303	54	chloroform	theory
	9a \rightarrow 10a	7.4 ^d	11.1	273–378	0.005	isooctane
8.0		12.3	273–378	0.03	isooctane	theory
3.0		8.2	245–309	0.009	isooctane	23
8.2		12.4	245–309	0.03	isooctane	theory
8.2		12.5	293–303	0.03	isooctane	theory
12 \rightarrow 13		4.2	8.3	293–334	0.002	isooctane
	11.5	12.5	293–334	0.0001	isooctane	theory
	11.5	12.4	293–303	0.0001	isooctane	theory

^a Theoretical results are CVT/SCT computed using HDFT+SM (HDFT \equiv mPW1PW91/6-31+G(d,p) and SM \equiv SM5.42R/HF/6-31G(d)//mPW1PW91/6-31+G(d,p)); E_a and $E_a^{V/T}$ in kcal/mol; A and $A^{V/T}$ in s^{-1} ; T in K; k_{298} in $10^8 s^{-1}$. ^b References are given for experimental results; theoretical results are from the present study. ^c Corrections for reaction with the solvent were included. ^d Corrections for a second-order reaction were included.

The reason solvation has a smaller effect on $E_a^{V/T}$ than on E_a^\ddagger is apparent from the fact that the values of κ in Table 5 are smaller for the reactions in solution than in the gas phase. Lowering the effective barrier height by selective solvation of the transition structure has a larger effect on increasing the rate of passage over the barrier than on increasing the rate of tunneling through it. By lowering the effective barrier height, solvation makes the top of the effective barrier broader and hence decreases the ability of tunneling to compete with overbarrier processes. This effect of solvation on the width of the barrier can be seen in Table 5 in the values of the imaginary frequency (ω^\ddagger) at the saddle point. A lower value for the imaginary frequency means a broader barrier, which makes tunneling through the barrier less competitive with passage over it.

The rate constants at 298 K, with and without tunneling, are also given in Table 5. The rate constants and the KIE, computed at different temperatures, are compared with the measured values in Table 2. The calculated rate constants change much more with temperature than the rate constants that have been measured. This difference reflects the difference, shown in Table 6, between the calculated values of $E_a^{V/T}$ and the much smaller experimental values of E_a . As also shown in Table 6, the calculated values of the preexponential factor, $A^{V/T}$, are much larger than the experimental values A . However, at 298 K the higher value of $A^{V/T}$ nearly compensates for the higher value of $E_a^{V/T}$; so the computed and measured rate constants differ by only a factor of 2 at this temperature.

The results in Table 2 reveal that our calculated KIEs do not agree with the experimental values either. The calculated KIE of $k_H/k_D = 11$ for the rearrangement of **2** to **3** in 1,2-dichloroethane at 248 K is more than an order of magnitude

TABLE 7: Gas-Phase Barrier Heights (V^\ddagger) and Energy of Reaction (ΔE) Computed at Various Levels of Theory for the Rearrangement of Methylchlorocarbene ($2 \rightarrow 3$)^a

method	V^\ddagger	ΔE
mPW1PW91/6-31+G(d,p)	12.6	-58.0
MPW1K/6-31+G(d,p)	13.5	-58.5
B3LYP/6-31+G(d,p)	13.9	-56.8
B3LYP/6-31G(d)	15.1	-57.7
MP2/6-31G(d)	13.6	-64.3
MP4/6-311+G(d,p)/MP2(FC)/6-31G(d,p) ^b	13.9	-58.0
QCISD(T)/6-311G(d,p)/MP2(FC)/6-31G(d,p) ^b	14.9	-56.8
CBS-Q/MP2/6-31G(d)	13.7	-58.5
CBS-Q/MPW1K/6-31+G(d,p)	13.7	-58.5
CBS-Q/mPW1PW91/6-31+G(d,p)	13.6	-58.6
CBS-Q/MC-QCISD	13.7	-58.4
MCG3/MC-QCISD	13.7	-57.8
MC-QCISD//ML	13.5	-57.9
MCG3//ML	13.9	-57.9

^a Values are in kcal/mol. ^b Ref 139.

larger than the experimental value of $k_H/k_D = 0.9$. Moreover, the calculated KIEs behave in the fashion typically observed for large KIEs, i.e., they decrease with increasing temperature. In contrast, as already noted, the measured values show the opposite behavior; they increase with increasing temperature.

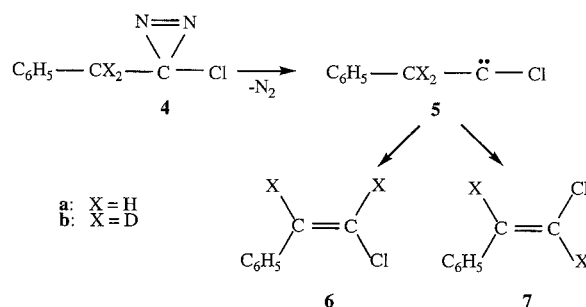
Our computed KIEs for the rearrangement of **2** to **3** are more similar to the experimental values reported for the rearrangement of dimethylcarbene to propene.^{27,52} At room temperature in pentane Modarelli et al.²⁷ reported a KIE of 3.2, based on the lifetime of deuterated dimethylcarbene compared to the undeuterated one. Ford et al.⁵² also found that tunneling contributions in the deuterated system are much smaller than in the undeuterated carbene. In addition, a KIE of 5 has been reported for the 1,2-H versus 1,2-D shift in neopentylfluorocarbene at ambient temperature in pentane.²⁹

Since Table 6 shows that our calculations give values of E_a that are ca. 2 kcal/mol higher than the experimental value, we decided to investigate whether higher-level electronic structure calculations might significantly lower the computed barrier height. Although tests on a suite of reactions (mostly H transfers) had led us to expect that mPW1PW91 and MPW1K should yield more accurate barrier heights than B3LYP,⁸⁶ we also carried out B3LYP/6-31+G(d,p) calculations. As shown in Table 7, these calculations gave $V^\ddagger = 13.9$ kcal/mol, which is *higher* than the values of $V^\ddagger = 12.6$ and 13.5 kcal/mol given by mPW1PW91 and MPW1K.

The highest-level ab initio calculations on the rearrangement of **2** to **3** that have been reported previously are the MP4/6-311+G(d,p)/MP2(FC)/6-31G(d,p) and QCISD(T)/6-311G(d,p)/MP2(FC)/6-31G(d,p) calculations by Riehl and Morokuma,¹³⁹ which yielded V^\ddagger values of 13.9 and 14.9 kcal/mol, respectively. These values are also both higher, not lower, than the mPW1PW91 and MPW1K values.

To assess the possible effects of higher levels of electron correlation and even larger basis sets, we also calculated the barrier height by two classes of methods that employ extrapolation to complete CI, namely the so-called complete basis set (CBS) scheme⁹¹ and the multi-coefficient correlation method (MCCM) schemes.⁹²⁻⁹⁶ For the CBS scheme we carried out single-point energy evaluations by the CBS-Q method.⁹¹ The results, which are given in Table 7, show that CBS-Q gives barriers which are about 1 kcal/mol higher than those computed by mPW1PW91, which is the HDFT method that we used for most of our dynamical calculations.

Finally, we carried out calculations in which we optimized the reactant and transition state structures by two MCCM

SCHEME 2

methods that should be much more accurate. MC-QCISD//ML calculations^{92,93} yielded $V^\ddagger = 13.5$ kcal/mol and MCG3//ML calculations⁹³⁻⁹⁵ yielded $V^\ddagger = 13.9$ kcal/mol. These calculations are expected to be very reliable, and the results obtained from them should erase all doubts that convergence in the electronic structure calculations is a problem.¹⁴⁰

3.3. 1,2-Hydrogen Migration in Benzylchlorocarbene. The 1,2-hydrogen shift in benzylchlorocarbene (**5**) gives rise to *Z*- and *E*- β -chlorostyrenes (**6** and **7**, respectively, in Scheme 2). For more than a decade much effort has been devoted to studying this reaction.^{12,13,16,19,24,30-32,36,42,46,54} It has been suggested that the kinetic analysis can be complicated by the intervention of a carbene-alkene complex,^{12,16,24} by hydrogen migration occurring concurrently with nitrogen elimination in an excited state of the 3-benzyl-3-chlorodiazirine (**4**),³¹ by the reaction of benzylchlorocarbene with the parent benzylchlorodiazirine,^{46,54} and/or by the insertion reaction of benzylchlorocarbene into C-H bonds of the solvent.^{42,54} The reported kinetic parameters, especially those from the earliest studies, may contain errors due to these side reactions. However, recent studies with non-nitrogenous carbene precursors indicate that carbene-alkene complexes are unlikely to intervene in the rearrangement of benzylchlorocarbene and thus complicate the observed kinetics.⁵¹

One early study²⁴ reported Arrhenius activation energies for 1,2-hydrogen migration in **5** to be 4.5 to 4.8 kcal/mol in isooctane. The experimental activation energy in isooctane increased to 5.8 kcal/mol when corrections for the side reaction of the carbene with the solvent were included, and $E_a = 3.6$ kcal/mol was found in chloroform.⁴² More recently,⁵⁴ it was stated that side reactions make the low-temperature data unsuitable for extracting Arrhenius parameters in both isooctane and methylcyclohexane. However, an Arrhenius activation energy of 3.2 kcal/mol was measured in 1,1,2,2-tetrachloroethane, where the side reactions are apparently insignificant.

As in a B3LYP/6-31G(d) study by Keating et al.,⁶⁹ at the mPW1PW91/6-31+G(d,p) level of electronic structure theory we found two stable conformers for the benzylchlorocarbene. The conformer with the slightly lower electronic energy has the phenyl group face-on to the empty carbene *p* orbital, but the inclusion of the zero-point energy favors the conformer in which the phenyl and chlorine are anti. This latter conformer was used as the reactant in the dynamics calculations. The results are presented in Tables 8 and 9.

The saddle point for the 1,2-hydrogen migration that gives rise to the *E* isomer (**7**) of β -chlorostyrene is lower in energy than the saddle point that leads to the *Z* isomer by about 2.4 kcal/mol in the gas phase and just slightly less in isooctane and chloroform. The addition of zero-point energy results in small increases in these differences. Accordingly, the kinetic parameters (Table 8) and the calculated rate constants (Table 9) for the 1,2-hydrogen migration are dominated by the rearrangement

TABLE 8: Energetic and Kinetic Parameters for the Benzylchlorocarbene Rearrangement^a

reaction	ΔE	V^\ddagger	ΔH_0^\ddagger	ΔH_{298}^\ddagger	ΔS_{298}^\ddagger	E_a^\ddagger	A^\ddagger	$\Delta H_{298}^{V/T}$	$\Delta S_{298}^{V/T}$	$E_a^{V/T}$	$A^{V/T}$
HDFT ^b											
5a → 6a	-62.6	9.0	7.6	7.3	-2.4	7.8	5.0(12) ^c	6.0	-4.8	6.6	1.5(12)
5a → 7a	-63.5	6.6	4.9	4.7	-3.1	5.3	3.5(12)	3.7	-4.9	4.3	1.4(12)
5a → 6a + 7a				4.7	-2.9	5.3	3.9(12)	3.8	-4.7	4.3	1.6(12)
5b → 6b	-62.6	9.0	8.1	7.7	-2.7	8.3	4.3(12)	7.1	-3.9	7.7	2.3(12)
5b → 7b	-63.5	6.6	5.5	5.2	-3.4	5.8	3.1(12)	4.6	-4.4	5.2	1.8(12)
5b → 6b + 7b				5.3	-3.2	5.9	3.4(12)	4.7	-4.2	5.3	2.0(12)
HDFT+SM ^d (isooctane)											
5a → 6a	-63.2	7.5	6.1	5.8	-2.3	6.4	5.2(12)	5.0	-3.9	5.6	2.3(12)
5a → 7a	-64.1	5.2	3.5	3.3	-3.1	3.9	3.5(12)	2.7	-4.4	3.3	1.9(12)
5a → 6a + 7a				3.4	-2.9	4.0	3.9(12)	2.7	-4.1	3.3	2.1(12)
5b → 6b	-63.2	7.5	6.6	6.3	-2.6	6.9	4.6(12)	5.8	-3.4	6.4	3.0(12)
5b → 7b	-64.1	5.2	4.1	3.9	-3.2	4.5	3.3(12)	3.4	-4.0	4.0	2.2(12)
5b → 6b + 7b				3.9	-3.0	4.5	3.7(12)	3.5	-3.8	4.1	2.5(12)
HDFT+SM ^d (chloroform)											
5a → 6a	-63.3	6.7	5.3	5.2	-2.3	5.8	5.3(12)	4.5	-3.7	5.1	2.7(12)
5a → 7a	-64.2	4.6	3.0	2.9	-3.1	3.5	3.6(12)	2.3	-4.2	2.9	2.1(12)
5a → 6a + 7a				2.9	-2.8	3.5	4.1(12)	2.3	-3.9	2.9	2.4(12)
5b → 6b	-63.3	6.7	5.8	5.6	-2.5	6.2	4.7(12)	5.2	-3.3	5.8	3.3(12)
5b → 7b	-64.2	4.6	3.6	3.4	-3.3	4.0	3.3(12)	3.0	-4.0	3.6	2.3(12)
5b → 6b + 7b				3.4	-3.0	4.0	3.8(12)	3.1	-3.7	3.7	2.7(12)

^a ΔE , V^\ddagger , ΔH_0^\ddagger , ΔH_{298}^\ddagger , $\Delta H_{298}^{V/T}$, E_a^\ddagger , and $E_a^{V/T}$ in kcal/mol; ΔS_{298}^\ddagger and $\Delta S_{298}^{V/T}$ in cal mol⁻¹ K⁻¹; A^\ddagger and $A^{V/T}$ in s⁻¹. ^b HDFT ≡ mPW1PW91/6-31+G(d,p). ^c 5.0(12) ≡ 5.0 × 10¹². ^d SM ≡ SM5.42R/HF/6-31G(d)/mPW1PW91/6-31+G(d,p).

TABLE 9: Rate Constants (s⁻¹), SCT Transmission Coefficients, and the Imaginary Frequency (cm⁻¹) at the Saddle Point for the 1,2-Hydrogen Rearrangement of Benzylchlorocarbene at 298 K

compound	k^{CVT}	$k^{V/T}$	κ	ω^\ddagger
HDFT ^a				
5a → 6a	8.8(6) ^b	2.1(7)	2.4	900 <i>i</i>
5a → 7a	4.7(8)	9.9(8)	2.1	873 <i>i</i>
5a → 6a + 7a	4.8(8)	1.0(9)	2.1	
5b → 6b	3.5(6)	5.6(6)	1.6	681 <i>i</i>
5b → 7b	1.7(8)	2.6(8)	1.6	673 <i>i</i>
5b → 6b + 7b	1.7(8)	2.7(8)	1.6	
HDFT+SM ^c (isooctane)				
5a → 6a	9.8(7)	1.8(8)	1.9	
5a → 7a	4.5(9)	7.7(9)	1.7	
5a → 6a + 7a	4.6(9)	7.9(9)	1.7	
5b → 6b	4.1(7)	5.7(7)	1.4	
5b → 7b	1.7(9)	2.4(9)	1.4	
5b → 6b + 7b	1.8(9)	2.5(9)	1.4	
HDFT+SM ^c (chloroform)				
5a → 6a	3.0(8)	5.3(8)	1.7	
5a → 7a	1.0(10)	1.6(10)	1.6	
5a → 6a + 7a	1.1(10)	1.7(10)	1.6	
5b → 6b	1.3(8)	1.7(8)	1.4	
5b → 7b	3.9(9)	5.3(9)	1.3	
5b → 6b + 7b	4.0(9)	5.4(9)	1.3	

^a HDFT ≡ mPW1PW91/6-31+G(d,p). ^b 4.1(3) ≡ 4.1 × 10³. ^c SM ≡ SM5.42R/HF/6-31G(d)/mPW1PW91/6-31+G(d,p).

to the *E* product (reaction **5** → **7**). At 298 K the *E/Z* product distribution is calculated to be about 98:2 both in the gas phase and in solution. Experimentally, in the photolysis of benzylchlorodiazirine, depending on the exact experimental conditions, the *E/Z* ratio varies between 1.5 and 5.1,^{12,24,31,54} although some smaller values have also been reported.^{16,31} Higher values have been obtained for the thermolysis of substituted benzylchlorodiazirines¹⁶ and 3-benzyl-3-bromodiazirine.¹⁴

Stabilization by the phenyl group of the transition structure for the lower energy 1,2-hydrogen shift makes $E_a^{V/T}$ for the rearrangement of **5a** to **7a** only about half as large as the corresponding values of $E_a^{V/T}$ for the rearrangement of **2a** to **3a**. Solvent effects reduce both the classical and zero-point-inclusive barrier heights for the rearrangement of **5a** by 1.4–

2.3 kcal/mol. Because the barrier height for the rearrangement of **5a** is smaller than that for the rearrangement of **2a**, it is not surprising that the magnitude of the imaginary frequency is smaller and that the calculated hydrogen tunneling contributions are not as large for **5a** as for **2a**. The transmission coefficients of 2.4 for **5a** → **6a** and 2.1 for **5a** → **7a** in the gas phase (Table 9) are only about a third the size of that for **2a** → **3a** (Table 5). The values of κ in the liquid phase for the rearrangement of **5** are smaller than 2.

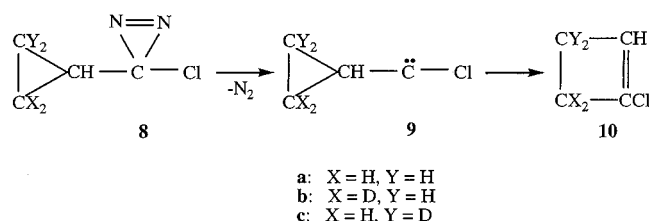
In the gas phase, tunneling effects are calculated to reduce the apparent Arrhenius activation energy for a 1,2-hydrogen shift in **5** by about 1 kcal/mol and to make the entropy of activation more negative by about 2 cal mol⁻¹ K⁻¹ (Table 8). The tunneling effects are calculated to be smaller in the liquid phase.¹⁴¹ As expected, the tunneling contributions to the rearrangement rates are computed to be smaller for the deuterated carbene (**5b**) than for the undeuterated carbene (**5a**).

The rearrangement of the deuterated carbene has been investigated experimentally in isooctane and chloroform.⁴² In isooctane, Liu et al.⁴² found that the KIE is 2.4 at 293 K and that it *increases* with increasing temperature. This type of temperature dependence of a KIE is unusual, but it is similar to the temperature dependence observed for the KIE in methylchlorocarbene³⁴ and discussed in the previous section. When correction for a parallel reaction was considered, the experimental KIE was measured to be between 3.5 and 4.0 in isooctane. In chloroform the experiments of Liu et al.⁴² yield a value of 2.7 for k_H/k_D .

The calculated deuterium KIEs (based on $k^{V/T}(298)$ for **5a** and **5b** in Table 9) are $k_H/k_D = 3.8$ in the gas phase, 3.2 in isooctane, and 3.1 in chloroform for the rearrangement that produces both the *Z* and *E* isomers. Thus our calculations give reasonably good agreement with the experimental values for the KIE at 298 K. Similar to the results we obtained for the hydrogen migration in methylchlorocarbene, the calculated KIEs decrease with increasing temperature.

In contrast to the case for the rearrangement of methylchlorocarbene (**2**) in *n*-heptane, for which the calculated rate constants are smaller than those measured at all temperatures (Table 2), for the rearrangement of **5a** in isooctane the calculated

SCHEME 3



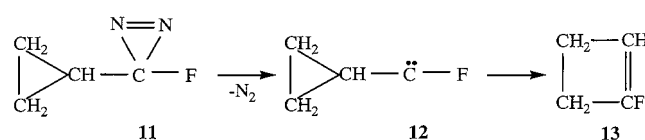
$k^{V/T}$ rate constant at 298 K is 2 orders of magnitude larger than those that have been measured (Table 6). As also shown in Table 6, in isooctane, this is due to the fact that the calculated value of $E_a^{V/T}$ is 1.2–2.5 kcal/mol lower than the values of E_a that have been measured. In chloroform $E_a^{V/T}$ is only 0.7 kcal/mol smaller than E_a , but the calculated value of $A^{V/T}$ is 2 orders of magnitude larger than the experimental value of A .

3.4. 1,2-Methylene Migration in Cyclopropylchlorocarbene and Cyclopropylfluorocarbene. Although 1,2-hydrogen shifts could, in principle, occur in the cyclopropylhalocarbenes, in fact, 1,2-methylene migration dominates and leads to the formation of 1-halocyclobutenes. Liu and Bonneau²² first reported the kinetic parameters for the ring expansion rearrangement of cyclopropylchlorocarbene (**9** in Scheme 3) to 1-chlorocyclobutene (**10**). Their values, $E_a = 7.4$ kcal/mol and $\log A = 11.1$ in isooctane, were obtained by direct observation of the carbene and contained corrections for carbene dimerization, which is kinetically a second-order process.

Moss et al.²³ measured the rate of rearrangement of **9** in isooctane by four different techniques under conditions where they found carbene dimerization to be unimportant. Their experiments led to $E_a = 2.8$ – 3.8 kcal/mol, with $\log A = 8.0$ – 8.7 . These values of E_a and $\log A$ are significantly lower than those reported by Liu and Bonneau.²² However, conversion of both sets of experimental activation parameters to free energies of activation affords, in each case, a value of about $\Delta G_{\text{act}} = 9$ kcal/mol at 298 K. The reported rate constants in both studies were between $k = 4 \times 10^5$ and $9 \times 10^5 \text{ s}^{-1}$ at temperatures between 289 and 301 K.^{20,22,23,28}

The rearrangement of cyclopropylfluorocarbene (**12** in Scheme 4) to 1-fluorocyclobutene (**13**) in isooctane was found by Moss et al.²⁸ to have kinetic parameters similar to those measured

SCHEME 4



for the rearrangement of **9** to **10**. The measured values were $E_a = 4.2$ kcal/mol, $A = 10^{8.3} \text{ s}^{-1}$, and $k = 1.4 \times 10^5 \text{ s}^{-1}$ at 293 K.²⁸

The mPW1PW91/6-31+G(d,p) barrier heights (Table 10) are appreciably different for the rearrangements of **9** and **12**; and, as expected from the better π electron donating ability of F compared to Cl, the barrier for **12** is higher. For the gas-phase rearrangements these HDFT calculations yield zero-point-inclusive barrier heights of $\Delta H_0^\ddagger = 10.4$ kcal/mol for the chlorocarbene (**9**) and $\Delta H_0^\ddagger = 14.3$ for the fluorocarbene (**12**). The HDFT activation enthalpy for the rearrangement of **9** is about 2 kcal/mol larger than that computed at the HF/6-311G(d)//HF/6-31G(d) level by Krogh-Jespersen, Moss, and co-workers.²⁰

As shown in Table 10, solvation effects reduce the activation enthalpies. For the rearrangement of the chlorocarbene, the calculated reduction amounts to about 2 kcal/mol in isooctane and 3 kcal/mol in chloroform. For the rearrangement of the fluorocarbene, each calculated reduction is 0.5–1.0 kcal/mol larger. These large reductions are understandable since Table 4 shows that in both carbene rearrangements the liquid-phase dipole moment of the transition states are 1.5–1.6 D larger than that of the reactants. Although the square of the dipole moment increases by about the same amount in both reactions, solvation is computed to have an appreciably larger effect on the rearrangement of **12** than of **9** because the solvation free energy depends on the full charge distribution, not just its lowest nonzero multiple moment.

We dissected the solvent effects on the rates into two components, one from bulk electrostatics and one from the nonbulk effects from molecules in the first solvation shell. In the rearrangements of both **9** and **12**, contributions from molecules in the first solvation shell speed up the reactions by a factor between 4.5 and 5.2 (0.9–1.0 kcal/mol). Almost all of the variability in the solvent effects on the rates comes from

TABLE 10: Energetic and Kinetic Parameters for the Cyclopropylhalocarbene Rearrangements^a

reaction	ΔE	V^\ddagger	ΔH_0^\ddagger	ΔH_{298}^\ddagger	ΔS_{298}^\ddagger	E_a^\ddagger	A^\ddagger	$\Delta H_{298}^{V/T}$	$\Delta S_{298}^{V/T}$	$E_a^{V/T}$	$A^{V/T}$
HDFT ^b											
9a → 10a	-52.0	11.1	10.4	10.1	-2.8	10.7	4.1(12) ^c	9.7	-3.6	10.3	2.7(12)
9b → 10b	-52.0	11.1	10.5	10.2	-2.9	10.8	4.0(12)	9.8	-3.6	10.4	2.8(12)
9c → 10c	-52.0	11.1	10.4	10.1	-2.9	10.7	4.0(12)	9.7	-3.7	10.3	2.7(12)
HDFT+SM ^d (isooctane)											
9a → 10a	-52.2	8.9	8.2	7.9	-2.8	8.5	4.1(12)	7.6	-3.4	8.2	3.0(12)
9b → 10b	-52.2	8.9	8.3	8.0	-2.8	8.6	4.0(12)	7.7	-3.4	8.3	3.1(12)
9c → 10c	-52.2	8.9	8.2	7.9	-2.9	8.5	4.0(12)	7.6	-3.4	8.2	3.0(12)
HDFT+SM ^d (chloroform)											
9a → 10a	-51.9	7.9	7.2	7.0	-2.8	7.5	4.1(12)	6.7	-3.3	7.3	3.2(12)
9b → 10b	-51.9	7.9	7.3	7.0	-2.8	7.6	4.1(12)	6.8	-3.3	7.4	3.2(12)
c → 10c	-51.9	7.9	7.2	6.9	-2.9	7.5	4.0(12)	6.7	-3.3	7.3	3.1(12)
HDFT ^b											
12 → 13	-48.2	15.0	14.3	14.0	-2.8	14.6	4.0(12)	13.4	-3.9	14.0	2.4(12)
HDFT+SM ^d (isooctane)											
12 → 13	-48.6	12.4	11.6	11.3	-2.8	11.9	4.1(12)	10.9	-3.6	11.5	2.7(12)
HDFT+SM ^d (chloroform)											
12 → 13	-48.5	11.0	10.3	9.9	-2.8	10.5	4.1(12)	9.6	-3.5	10.2	2.9(12)

^a ΔE , V^\ddagger , ΔH_0^\ddagger , ΔH_{298}^\ddagger , $\Delta H_{298}^{V/T}$, E_a^\ddagger , and $E_a^{V/T}$ in kcal/mol; ΔS_{298}^\ddagger and $\Delta S_{298}^{V/T}$ in cal mol⁻¹ K⁻¹; A^\ddagger and $A^{V/T}$ in s⁻¹. ^b HDFT ≡ mPW1PW91/6-31+G(d,p). ^c 4.1(12) ≡ 4.1×10^{12} . ^d SM ≡ SM5.42R/HF/6-31G(d)/mPW1PW91/6-31+G(d,p).

TABLE 11: Rate Constants (s^{-1}), SCT Transmission Coefficients, and the Imaginary Frequency (cm^{-1}) at the Saddle Point for the 1,2-Carbon Rearrangements in Cyclopropylhalocarbenes at 298 K

compound	k^{CVT}	k^{VT}	κ	ω^\ddagger
HDFT ^a				
9a → 10a	5.5(4) ^b	7.8(4)	1.4	604 <i>i</i>
9b → 10b	4.8(4)	6.6(4)	1.4	579 <i>i</i>
9c → 10c	5.7(4)	8.0(4)	1.4	601 <i>i</i>
HDFT+SM ^c (isooctane)				
9a → 10a	2.2(6)	2.9(6)	1.3	
9b → 10b	1.9(6)	2.4(6)	1.3	
9c → 10c	2.3(6)	2.9(6)	1.3	
HDFT+SM ^c (chloroform)				
9a → 10a	1.2(7)	1.5(7)	1.2	
9b → 10b	1.0(7)	1.2(7)	1.2	
9c → 10c	1.2(7)	1.5(7)	1.2	
HDFT ^a				
12 → 13	8.3(1)	1.3(2)	1.5	663 <i>i</i>
HDFT+SM ^c (isooctane)				
12 → 13	7.7(3)	1.1(4)	1.4	
HDFT+SM ^c (chloroform)				
12 → 13	7.4(4)	1.0(5)	1.3	

^a HDFT ≡ mPW1PW91/6-31+G(d,p). ^b 5.5(4) ≡ 5.5 × 10⁴. ^c SM ≡ SM5.42R/HF/6-31G(d)//mPW1PW91/6-31+G(d,p).

bulk electrostatics, which contributes a speedup as small as a factor of 9 (for the chlorocarbene in isooctane, where the differential solvation energy between transition state and reactant is 1.3 kcal/mol) or as large as a factor of 173 (for fluorocarbene in chloroform, where the effect is 3.1 kcal/mol).

Tunneling effects are not appreciable in either reaction. As shown in Table 10, tunneling is calculated to reduce the apparent Arrhenius activation energies by only about 0.5 kcal/mol and to make the entropies of activation more negative by less than 1 cal mol⁻¹ K⁻¹. The transmission coefficients, which are given in Table 11, are calculated to be less than 1.5 in both reactions at 298 K.

We computed the secondary deuterium KIE for CH₂ versus CD₂ migration in the rearrangement of cyclopropylchlorocarbene-*d*₂ (**9c/9b**). Moss et al.³⁸ have measured this KIE in deuterated chloroform. Our calculations for chloroform give secondary KIEs of $k_H/k_D = k^{VT}(\mathbf{9c} \rightarrow \mathbf{10c})/k^{VT}(\mathbf{9b} \rightarrow \mathbf{10b}) = 1.25, 1.20, \text{ and } 1.17$ at 243, 294, and 333 K, respectively. These calculated ratios are in excellent agreement with the experimental values of 1.28, 1.20, and 1.18.³⁸ Similar ratios are also obtained if the KIEs are calculated from TST. For the gas phase, values of $k^{TST}(\mathbf{9c} \rightarrow \mathbf{10c})/k^{TST}(\mathbf{9b} \rightarrow \mathbf{10b}) = 1.23, 1.19, \text{ and } 1.16$ at 243, 294, and 333 K, respectively, are computed. Since the TST calculations do not include tunneling corrections, this good agreement between the two sets of calculated k_H/k_D values shows again that tunneling is not computed to be significant in this reaction.

Table 6 shows that, for the rearrangement of cyclopropylchlorocarbene (**9a** → **10a**), the kinetic parameters that we have calculated are much more similar to those reported by Liu and Bonneau²² than to those reported by Moss et al.²³ For the rearrangement of cyclopropylfluorocarbene (**12** → **13**), the values computed by us and those measured by Moss and co-workers disagree even more. As shown in Table 6, the value of E_a^{VT} that we have computed for the rearrangement of **12** to **13** in isooctane is more than 7 kcal/mol larger than the value of E_a measured by Moss and co-workers in this solvent; and the calculated value of A^{VT} is about 4 orders of magnitude larger than the experimental value of A .

TABLE 12: Gas-Phase Barrier Heights (V^\ddagger), Activation Enthalpies (ΔH_{298}^\ddagger), and Activation Entropies (ΔS_{298}^\ddagger) Computed at Various Levels of Theory for the Rearrangement of Cyclopropylfluorocarbene (12** → **13**)^a**

method	V^\ddagger	ΔH_{298}^\ddagger	ΔS_{298}^\ddagger
mPW1PW91/6-31+G(d,p)	15.0	14.0	-2.8
MPW1K/6-31+G(d,p)	16.3	15.3	-2.9
B3LYP/6-31+G(d,p)	15.7	14.7	-2.6
B3LYP/6-31G(d)	16.6	15.6	-2.6
MP2/6-31G(d)	16.0	14.8	-2.9
(10/10)/CASSCF/6-31G(d)	18.6	17.6	-2.7
(10/10)/CASPT2/6-31G(d)//CASSCF/6-31G(d)	18.1	17.1 ^b	
(10/10)/CASPT2/cc-pVTZ//CASSCF/6-31G(d)	15.7	14.7 ^b	
CBS-Q//CASSCF/6-31G(d)	15.5	14.5 ^b	
CBS-Q//mPW1PW91/6-31+G(d,p)	15.7	14.6 ^c	
CBS-APNO//CASSCF/6-31G(d)	15.2	14.2 ^b	
CBS-APNO//mPW1PW91/6-31+G(d,p)	15.3	14.3 ^c	
MC-QCISD//CASSCF/6-31G(d)	15.6	14.6 ^b	
MC-QCISD//mPW1PW91/6-31+G(d,p)	15.8	14.7 ^c	
MCG3//CASSCF/6-31G(d)	14.5	13.5 ^b	
MCG3//mPW1PW91/6-31+G(d,p)	15.0	14.0 ^c	

^a V^\ddagger and ΔH_{298}^\ddagger in kcal/mol; ΔS_{298}^\ddagger in cal mol⁻¹ K⁻¹. ^b Computed with (10/10)/CASSCF/6-31G(d) frequencies. ^c Computed with mPW1PW91/6-31+G(d,p) frequencies.

The very large difference between the computed and measured activation parameters for the rearrangement of **12** to **13** led us to investigate whether a very different set of activation parameters might be obtained if the transition structure were located and its energy computed with other types of electronic structure calculations. Therefore, we performed calculations with different hybrid density functional theory methods, namely B3LYP and MPW1K; we carried out (10,10)CASSCF calculations, followed by (10,10)CASPT2 single-point energy evaluations with two different basis sets; and we performed CBS-Q, CBS-APNO, MC-QCISD, and MCG3 single-point energy calculations. As shown in Table 12, none of the computed barrier heights is significantly lower than the one from the mPW1PW91/6-31+G(d,p) calculations. The generally good agreement of the additional high-level (CBS, MCG3, and CASPT2 with the largest basis) calculations in Table 12 with the mPW1PW91/6-31+G(d,p) calculations provides further evidence that the source of the disagreement between theory and experiment is not due to the inadequacy of the electronic structure calculations.

All of the methods in Table 12 give essentially the same value of ΔS_{298}^\ddagger as that computed by mPW1PW91/6-31+G(d,p). Therefore, like mPW1PW91/6-31+G(d,p), all of these other methods predict a value of the Arrhenius A factor for the rearrangement of **12** to **13** that is about 4 orders of magnitude larger than that obtained from the experiments of Moss and co-workers.

3.5. Further Discussion: The Transmission Coefficient. Moss,^{23,54} Platz,³³ and their co-workers have suggested that the small experimental A factors found in the 1,2-shifts of many carbenes are due to the fact that completion of these rearrangements requires rotation about the bond between the two carbons which serve as the migration origin and migration terminus. This rotation is necessary in order to allow formation of the π bond between these carbons in the product. It has been proposed that coupling of this rotation with the actual migration step might be relatively inefficient, resulting in most trajectories that cross the transition state being reflected back to the reactant, rather than reaching the product. Such a breakdown of transition state theory, both conventional and variational, could result in low transmission coefficients and, hence, in low A factors.

This suggestion is intriguing, and we have investigated it in

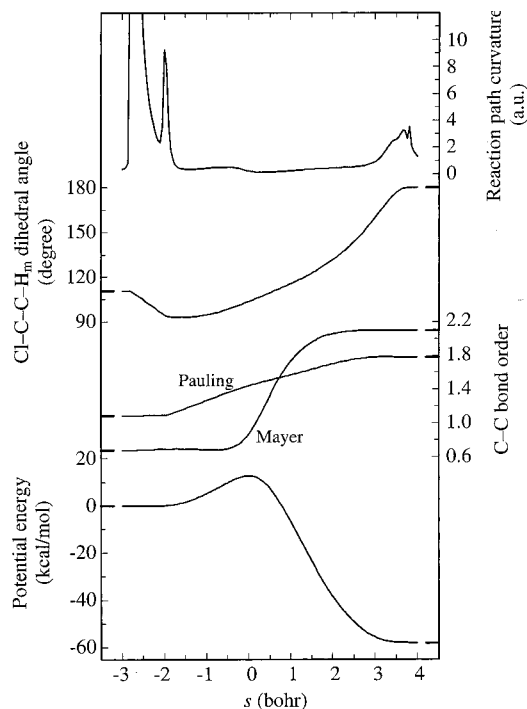


Figure 2. The reaction-path curvature, the Cl-C-C-H_m dihedral angle, the C-C bond order, and the potential energy along the gas-phase mPW1PW91/6-31+G(d,p) reaction coordinate for reaction R-1. The asymptotic values for the reactant and product are also represented.

more detail as presented below. However, even if such effects would rationalize the very low experimental *A* factor found in the rearrangement of **12** to **13**, they would not explain why the experimental *E_a* is at least 7 kcal/mol lower than the values predicted by all of our calculations. As a consequence of the difference between the experimental and calculated *E_a* values in isooctane, the experimental rate constant for **12** → **13** is 20 times larger than the calculated rate constant (Table 6) at 298 K. A low transmission coefficient could explain the difference between the experimental and calculated rate constants, but only if the former were smaller, not larger, than the latter.

For the rearrangement of methylchlorocarbene we have examined various geometrical parameters along the reaction path as well as the reaction-path curvature to determine whether the reaction path exhibits particularly sharp curves. As a benchmark for comparison, we note that the maximum value of the reaction path curvature is between 5.4 and 8.7 au for each of the six bimolecular hydrogen transfer reactions studied in a recent paper;¹⁴² these were “normal” reactions such as OH + CH₄ → H₂O + CH₃. With this background, we considered Figure 2, which shows that the reaction-path curvature is rather small except at geometries close to the reactant and to the product. It seems unlikely that these regions would be responsible for significant recrossings. The Cl-C-C-H_m (H_m represents the migrating hydrogen) dihedral angle, which was suggested to vary sharply during hydrogen migration in methylcarbene,³³ varies rather smoothly along the reaction path in this case (as also shown in Figure 2); and the other dihedral angles vary even more gradually. The C-C bond order also varies smoothly, as illustrated in Figure 2, whether calculated by the Pauling formalism¹⁴³ or the Mayer formalism.¹⁴⁴ However, whereas the Pauling bond order varies along the whole range of the reaction path (as a result of similar variation in the C-C bond distance), the Mayer bond order (which is a more realistic indication of bonding since it is based on the actual electron density) varies mostly on the product side of the reaction coordinate. Ultimately,

this analysis gives little reason to suspect unusually dramatic reaction-path curvature effects on the transmission coefficients.

In other possibly relevant work, Hayes et al.¹⁴⁵ calculated extensive short-time recrossing of the transition state region in the 1,2-deuterium migration reaction of CD₂=C: to form CD≡CD following sudden electron removal at 600 and 1440 K. It is hard to know whether one can infer a breakdown of transition state theory for calculations of thermal reaction rates from these calculations because of the choice of initial conditions and the lack of quantization in the vibrational modes.

4. Summary and Conclusions

The gas-phase barrier heights, calculated at various levels of electronic structure theory, are much higher than the experimentally determined, solution-phase Arrhenius activation energies for the 1,2-hydrogen migration in methylchlorocarbene (**2**) and for the 1,2-methylene migrations in cyclopropylchlorocarbene (**9**) and in cyclopropylfluorocarbene (**12**). The discrepancy is largest for the rearrangement of **12**. Such disagreements between theory and experiment for this class of reactions^{21,24,42,46,54,60,69} and for the closely related Wolff rearrangement¹⁴⁶ were also found in earlier work. In the latter study, consideration of heavy-atom tunneling (with a one-dimensional tunneling theory that is less reliable than the multidimensional theory used here) and solvation did not eliminate the disagreement. In the present study we systematically examined the following four possible reasons for this kind of disagreement in 1,2-hydrogen migrations and cyclopropylcarbene rearrangements: (i) inaccuracies in the electronic structure theory calculations, (ii) solvation, (iii) dynamical effects, and (iv) tunneling. As was found in the study of the Wolff rearrangement,¹⁴⁶ consideration of factors i, ii, and iv does not eliminate the disagreement with experiment, nor does consideration of dynamical effects.

We have performed the electronic structure calculations at high enough levels, including MCG3//ML and CASPT2/cc-pVTZ//CASSCF/6-31G(d), to rule out inaccuracies in these calculations as a major cause of the discrepancy. We did find that solvation reduces the effective barrier heights by 2–3 kcal/mol, with the effect being larger in chloroform than in hydrocarbon solvents. Solvation lowers the barrier heights because the increase in polarity on going from the reactant to the transition structure favors a medium with a high dielectric constant.

Quantum mechanical tunneling further reduces the gas-phase activation energy at 298 K for the 1,2-protium migration in methylchlorocarbene (**2a**) by almost 4 kcal/mol in our MP2/6-31G(d) calculations and by slightly more than 3 kcal/mol in our HDFT calculations. The corresponding reductions for 1,2-deuterium migration in methylchlorocarbene-*d*₃ (**2b**) are 1.7 and 1.4 kcal/mol, respectively. Figure 3 shows the Arrhenius representations of the CVT and CVT/SCT rate constants for the 1,2-protium migration and 1,2-deuterium migration in methylchlorocarbene and benzylchlorocarbene and for the 1,2-methylene migration in cyclopropylchlorocarbene and cyclopropylfluorocarbene, in all cases in isooctane solvent. These calculations are carried out in the separable equilibrium solvation (SES) approximation at the mPW1PW91/6-31+G(d,p) + GB level in which the solvation energy in isooctane is calculated using the GB approximation based on atomic charges determined using Löwdin population analysis of the mPW1PW91/6-31+G(d,p) wave function and is added to the potential energy along the gas-phase MEP by the ISPE-2 method. The Arrhenius activation parameters determined at this level for various

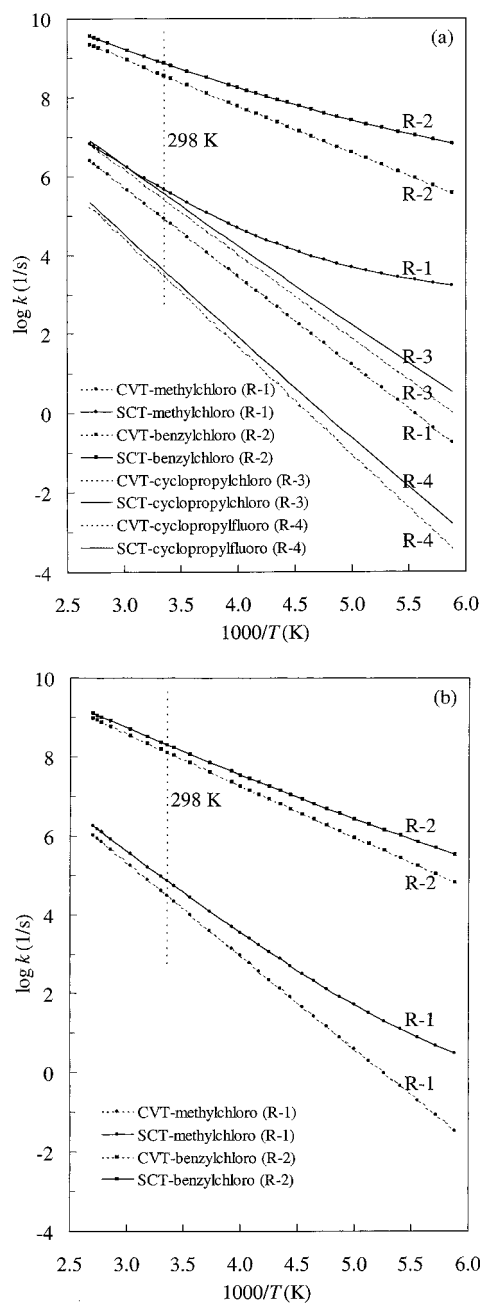


Figure 3. (a) Arrhenius representations of the calculated mPW1PW91/6-31+G(d,p)+GB CVT and CVT/SCT rate constants in isoctane over the 170–370 K range for the 1,2-protium migration in methylchloro-carbene and benzylchloro-carbene (sum of migrations to *Z*- and *E*-isomers) and for the 1,2-methylene migration in cyclopropylchloro-carbene and cyclopropylfluorocarbenes. (b) Same but for 1,2-deuterium migrations of **2b** → **3b** and **5b** → **6b** + **7b**.

temperatures are given in Table 1. The nonlinearity of the Arrhenius plot due to tunneling is visible at low temperatures for the 1,2-protium migration reactions but is insignificant for the 1,2-methylene migration reactions over the whole range of temperatures. Without tunneling, the nonlinearity is greatly reduced. The contribution of tunneling, relative to overbarrier reaction, is computed to be smaller in the liquid-phase reaction than in the gas-phase reaction, as a result of the smaller and hence broader barriers for rearrangement of **2** in solution.

Together, the effects of solvation and tunneling do decrease the disparity between the calculated and experimental activation parameters for the rearrangement of **2**; but, even together, these two effects do not fully account for all the differences between

the theoretical and experimental results. In addition, both the size and the temperature dependence of the computed KIEs are not just quantitatively, but are qualitatively different from those that have been measured for the rearrangement of **2**.

The phenyl moiety in the benzyl group in **5** lowers the gas-phase barrier height but also decreases the importance of solvation and tunneling in lowering the activation energy. It is noteworthy that, unlike the case in the rearrangement of **2**, inclusion of solvation effects and tunneling corrections makes the computed activation energy smaller (and the rate constant bigger) than the values that have been measured experimentally. Bringing yet one more system into the discussion, we note that theory⁶⁴ predicts a somewhat smaller rate constant than experiment²⁶ for methylphenylcarbene. There, however, solvent effects are predicted to result from the greater polarizabilities of transition states compared to reactants,⁶⁴ in contrast to the present case where the solvent effects apparently result mainly from greater polarities of the transition states compared to reactants.

In the rearrangements of cyclopropylhalocarbenes **9** and **12**, a methylene group migrates; and heavy-atom tunneling is computed to play a negligible role in these reactions. Previous calculations of tunneling contributions to the rates of 1,2-shifts have erroneously found that heavy atoms tunnel faster than light atoms in these reactions,⁶² leading to the suggestion³⁴ that heavy-atom tunneling might explain the low activation enthalpies and very negative activation enthalpies that have been found in these rearrangements. The results of our calculations appear to rule out this possibility. Heavy-atom tunneling was also calculated to be small in the Wolff rearrangement.¹⁴⁶

What, then, could account for the small activation enthalpies and very negative activation entropies found by Moss et al. in the rearrangements of **9** and **12**? One possible explanation, discussed in Section 3.4, is a breakdown of transition state theory, due to dynamical effects, that would result in small transmission coefficients.^{23,33,54,145} This could explain the low experimental *A* factors rather easily (although such a breakdown of transition state theory would be surprising), but there would have to be a very strong temperature dependence of the transmission coefficient to also explain the low values of E_a .

Another possible explanation of the anomalies in both of these activation parameters would be that the transition structures for these rearrangements bind one or more molecules of solvent much more tightly than the reactants do. This would reduce the activation enthalpies but make the activation entropies more unfavorable (i.e., negative). Especially when the halogen in the cyclopropylhalo-carbene is fluorine, halogen lone-pair donation into the empty *p* orbital of the carbene should reduce its electrophilicity, thus making it arguably less likely to coordinate a solvent molecule than the carbon to which a C–C bond is partially broken in the transition structure. In light of this possibility and the special problem of using nuclear-centered partial atomic charges for carbenes (noted above), some attempt to provide more definitive estimates of solvation effects would be desirable.

A problem with this explanation is that specific interactions between the transition structure and the solvent are unlikely to be strong in alkane solvents (or even in alkenes^{65,147}). A second problem with this explanation is that the SM5.42R solvation model does include specific interactions between a reacting molecule and the first shell of solvent molecules around it. The results of our calculations, using this model, do find that the calculated activation enthalpies are reduced by solvation, but much more by bulk than by specific solvation effects. This

reduction can easily be explained by the larger polarity of the transition structures as compared to the reactants.

In addition, even using the SM5.42R solvation model, the activation enthalpy for the rearrangement of **12** to **13** is still computed to be more than 7 kcal/mol higher than that measured by Moss and co-workers. Therefore, if the very low activation enthalpy for this rearrangement is due to selective stabilization of the transition structure by a strong interaction with solvent, the SM5.42R model grossly underestimates the strength of this interaction. Although there were no carbenes in the training set^{115,117} used to parametrize the model, and although we pointed out above that the partial atomic charges used in our solvation model systematically underestimate dipole moments, it seems unlikely that the SM5.42R solvation model is so inaccurate that it accounts for the majority of the error.

What possible experimental problems could lead to the large discrepancy, especially for **12**, between the computed activation parameters and those found experimentally? Since Moss et al. measured the activation parameters for the rearrangement of **9** by four independent methods, including direct observation of the disappearance of **9**, and since they obtained essentially the same set of activation parameters by all four methods,²³ many possibilities (e.g., a systematic error in following the rate of reaction, rearrangement occurring in an excited state of the carbene, and catalysis of the rearrangement by added carbene trapping reagent) can apparently be ruled out for reaction R-3. Nevertheless we do note that theory agrees much better with the results of the earlier experiments of Liu and Bonneau²² for reaction R-3, for which corrections for a second-order processes were considered.

Reaction conditions can have a large effect on carbene lifetimes for long-lived carbenes such as methylchlorocarbene or cyclopropylfluorocarbene. For example, trace amounts of water and oxygen reduce the lifetime of adamantylidene in benzene by an order of magnitude at ambient temperature.⁵⁵ However this is not expected to be a problem for short-lived carbenes.

Experimentally, the determination of the rate constant of 1,2-migrations in carbenes may be complicated by various concurrent reactions. For example, many investigations have obtained evidence that, at least in some cases, 1,2-atom migrations are concurrent with N₂ extrusion and occur from an excited state of diazirines,^{31,48–51,63} without the intermediacy of the carbene. Diazo compounds generated from diazirines have been ruled out as intermediates in the formation of olefins by 1,2-shifts because the formation of diazo compounds is unlikely at ambient temperature.⁴³ However, many studies have shown that the carbene may react with the parent diazirine to produce an azine.^{32,46,47} This reaction has been theoretically determined to be very favorable.⁷⁰ In addition, reaction of the carbene with an alkane solvent, leading to formation of C–H insertion products, has been shown to be significant in some cases.^{9,54} A priori, it seems possible that one of these or other reactions may increase the experimental values for the apparent rate constants for carbene disappearance, especially in the case of a carbene like **12**, which is predicted to have a relatively long lifetime.

The list of possible experimental pitfalls is indeed formidable, but close examination of the key experimental studies of carbenes **9a** and **12** shows that these problems were anticipated, and that they do not appear relevant in these cases.^{23,28} Thus, 1,2-migrations from excited states of diazirines do not bias the kinetic data, obtained either by direct observation of the carbene or by monitoring the pyridine ylide formed by reaction of the carbene with pyridine (in competition with carbene rearrange-

ment). Both of these methods were employed in the study of carbene **9a**, and the pyridine ylide method was used with carbene **12**.

Competitive, second-order, side reactions (such as azine formation, carbene dimerization, or carbene insertion into the solvent) can be real complications. However, in the case of **9a**, NMR product analysis of reactions, carried out between 255 and 294 K, demonstrated the formation of more than 90% of the 1-chlorocyclobutene expansion product (**10**), and less than 10% of possible dimerization or azine products. Capillary GC analysis confirmed 85–92% yields of **10**, with no evidence of carbene dimer.²³ For carbene **12**, a series of kinetics experiments was carried out at decreasing concentrations of the diazirine precursor, until an appropriate concentration was found at which deviations from first-order kinetics (possibly due to carbene dimer or azine formation) in the rates of pyridine ylide formation were absent. The formation of ring expansion product **13** was nearly quantitative.²⁸

In light of the discrepancy between the 1992 experimental value of E_a for the ring expansion of carbene **12** to fluorocyclobutene (4.2 kcal/mol)²⁸ and the value computed here (11.5 kcal/mol, Table 6), one of us and co-workers [R. A. Moss, F. Zheng, and Y. Ma] redetermined the experimental value. Three new, independent sets of rate constants vs inverse absolute temperature data (with temperature ranges of 253–313 K or 263–313 K) afforded $E_a = 5.1 \pm 1.1$ kcal/mol and $\log A = 9.2 \pm 0.9$ s⁻¹ in isoctane, in reasonable agreement with the 1992 report. The experimental activation energy is reproducible, and no obvious source of error is apparent.

Although this paper has focused on differences between calculations and experiments in 1,2-shifts in halocarbenes, we noted above that such discrepancies have also been found in the 1,2-migrations that occur in other types of carbenes. For example, Scott et al.¹⁴⁶ have observed that the computed barriers to Wolff rearrangements in carbonyl and alkoxy carbonyl carbenes are often much higher than those that have been measured. The disparity is particularly large for the Wolff rearrangement of carbomethoxychlorocarbene, and Scott et al.¹⁴⁶ discussed the possibility that the lifetime of this carbene may be controlled by bimolecular processes. This hypothesis may also ultimately prove to explain the same type of disparity between calculations and experiments that have been found in the rearrangements of cyclopropylchloro- and cyclopropylfluorocarbene and which have been discussed in this paper. It is, of course, also possible that these disparities are due to a factor or factors as yet unknown.

Acknowledgment. The authors are grateful to Joey Storer for discussions of his calculations, to Chris Cramer for many helpful interactions, to James Xidos for assistance with solvation calculations, and to Matt Platz for very helpful comments on the manuscript. We acknowledge the National Science Foundation for grants that partially supported this research.

Supporting Information Available: The Supporting Information includes geometries for all structures optimized in this work and further information about partial atomic charges. This material is available free of charge via the Internet at <http://pubs.acs.org>.

References and Notes

- (1) Bourissou, D.; Guerret, O.; Gabbai, F. P.; Bertrand, G. *Chem. Rev.* **2000**, *100*, 39.
- (2) Solet, S.; Gornitzka, H.; Schoeller, W. W.; Bourissou, D.; Bertrand, G. *Science (Washington, DC)* **2001**, *292*, 1901.

- (3) Nickon, A. *Acc. Chem. Res.* **1993**, *26*, 84.
- (4) Moss, R. A. In *Advances in Carbene Chemistry*; Brinker, U. H., Ed.; JAI Press Inc.: Greenwich, CT, 1994; Vol. 1, p 59.
- (5) Liu, M. T. H. *Acc. Chem. Res.* **1994**, *27*, 287.
- (6) Celebi, S.; Tsao, M.-L.; Platz, M. S. *J. Phys. Chem. A* **2001**, *105*, 1158.
- (7) Doyle, M. P.; Taunton, J.; Oon, S.-M.; Liu, M. T. H.; Soundararajan, N.; Platz, M. S.; Jackson, J. E. *Tetrahedron Lett.* **1988**, *29*, 5863.
- (8) Jones, M. B.; Maloney, V. M.; Platz, M. S. *J. Am. Chem. Soc.* **1992**, *114*, 2163.
- (9) Bonneau, R.; Liu, M. T. H. *J. Photochem. Photobiol. A* **1992**, *68*, 97.
- (10) Kirmse, W. In *Advances in Carbene Chemistry*; Brinker, U. H., Ed.; JAI Press Inc.: Greenwich, CT, 1994; Vol. 1, p 1.
- (11) Tomioka, H.; Okada, H.; Watanabe, T.; Banno, K.; Komatsu, K.; Hirai, K. *J. Am. Chem. Soc.* **1997**, *119*, 1582.
- (12) Tomioka, H.; Hayashi, N.; Izawa, Y.; Liu, M. T. H. *J. Am. Chem. Soc.* **1984**, *106*, 454.
- (13) Liu, M. T. H. *J. Chem. Soc., Chem. Commun.* **1985**, 982.
- (14) Liu, M. T. H.; Subramanian, R. *J. Phys. Chem.* **1986**, *90*, 75.
- (15) McMahon, R. J.; Chapman, O. L. *J. Am. Chem. Soc.* **1987**, *109*, 683.
- (16) Liu, M. T. H.; Soundararajan, N.; Paike, N.; Subramanian, R. *J. Org. Chem.* **1987**, *52*, 4223.
- (17) Bonneau, R.; Liu, M. T. H.; Rayez, M. T. *J. Am. Chem. Soc.* **1989**, *111*, 5973.
- (18) Liu, M. T. H.; Bonneau, R. *J. Am. Chem. Soc.* **1989**, *111*, 6873.
- (19) Jackson, J. E.; Soundararajan, N.; White, W.; Liu, M. T. H.; Bonneau, R.; Platz, M. S. *J. Am. Chem. Soc.* **1989**, *111*, 6874.
- (20) Ho, G. J.; Krogh-Jespersen, K.; Moss, R. A.; Shen, S.; Sheridan, R. S.; Subramanian, R. *J. Am. Chem. Soc.* **1989**, *111*, 6875.
- (21) LaVilla, J. A.; Goodman, J. L. *J. Am. Chem. Soc.* **1989**, *111*, 6877.
- (22) Liu, M. T. H.; Bonneau, R. *J. Phys. Chem.* **1989**, *93*, 7298.
- (23) Moss, R. A.; Ho, G. J.; Shen, S.; Krogh-Jespersen, K. *J. Am. Chem. Soc.* **1990**, *112*, 1638.
- (24) Liu, M. T. H.; Bonneau, R. *J. Am. Chem. Soc.* **1990**, *112*, 3915.
- (25) LaVilla, J. A.; Goodman, J. L. *Tetrahedron Lett.* **1990**, *31*, 5109.
- (26) Sugiyama, M. H.; Celebi, S.; Platz, M. S. *J. Am. Chem. Soc.* **1992**, *114*, 966.
- (27) Modarelli, D. A.; Morgan, S.; Platz, M. S. *J. Am. Chem. Soc.* **1992**, *114*, 7034.
- (28) Moss, R. A.; Ho, G. J.; Liu, W. *J. Am. Chem. Soc.* **1992**, *114*, 959.
- (29) Moss, R. A.; Ho, G. J.; Liu, W.; Sierakowski, C. *Tetrahedron Lett.* **1992**, *33*, 4287.
- (30) Liu, M. T. H.; Bonneau, R. *J. Am. Chem. Soc.* **1992**, *114*, 3604.
- (31) White, W. R., III; Platz, M. S. *J. Org. Chem.* **1992**, *57*, 2841.
- (32) Liu, M. T. H.; Chapman, R. G.; Bonneau, R. *J. Photochem. Photobiol. A* **1992**, *63*, 115.
- (33) Modarelli, D. A.; Platz, M. S. *J. Am. Chem. Soc.* **1993**, *115*, 470.
- (34) Dix, E. J.; Herman, M. S.; Goodman, J. L. *J. Am. Chem. Soc.* **1993**, *115*, 10424.
- (35) Modarelli, D. A.; Platz, M. S.; Sheridan, R. S.; Ammann, J. R. *J. Am. Chem. Soc.* **1993**, *115*, 10440.
- (36) Wierlacher, S.; Sander, W.; Liu, M. T. H. *J. Am. Chem. Soc.* **1993**, *115*, 8943.
- (37) Moss, R. A.; Ho, G. J. *J. Phys. Org. Chem.* **1993**, *6*, 126.
- (38) Moss, R. A.; Liu, W.; Krogh-Jespersen, K. *Tetrahedron Lett.* **1993**, *34*, 6025.
- (39) Moss, R. A.; Liu, W.; Krogh-Jespersen, K. *J. Phys. Chem.* **1993**, *97*, 13413.
- (40) Dix, E. J.; Goodman, J. L. *Res. Chem. Intermed.* **1994**, *20*, 149.
- (41) Chidester, W.; Modarelli, D. A.; White, W. R., III; Whitt, D. E.; Platz, M. S. *J. Phys. Org. Chem.* **1994**, *7*, 24.
- (42) Liu, M. T. H.; Bonneau, R.; Wierlacher, S.; Sander, W. *J. Photochem. Photobiol. A* **1994**, *84*, 133.
- (43) Bonneau, R.; Liu, M. T. H.; Kim, K. C.; Goodman, J. L. *J. Am. Chem. Soc.* **1996**, *118*, 3829.
- (44) Moss, R. A.; Xue, S.; Liu, W. G.; Krogh-Jespersen, K. *J. Am. Chem. Soc.* **1996**, *118*, 12588.
- (45) Shin, S. H.; Cizmeciyan, D.; Keating, A. E.; Khan, S. I.; Garcia-Garibay, M. A. *J. Am. Chem. Soc.* **1997**, *119*, 1859.
- (46) Moss, R. A.; Maksimovic, L.; Merrer, D. C. *Tetrahedron Lett.* **1997**, *38*, 7049.
- (47) Moss, R. A.; Merrer, D. C. *Chem. Commun.* **1997**, 617.
- (48) Pezacki, J. P.; Pole, D. L.; Warkentin, J.; Chen, T.; Ford, F.; Toscano, J.; Fell, J.; Platz, M. S. *J. Am. Chem. Soc.* **1997**, *119*, 3191.
- (49) Platz, M. S.; Huang, H.; Ford, F.; Toscano, J. *Pure Appl. Chem.* **1997**, *69*, 803.
- (50) Huang, H.; Platz, M. S. *J. Am. Chem. Soc.* **1998**, *120*, 5990.
- (51) Nigam, M.; Platz, M. S.; Showalter, B. M.; Toscano, J. P.; Johnson, R.; Abbot, S. C.; Kirchhoff, M. M. *J. Am. Chem. Soc.* **1998**, *120*, 8055.
- (52) Ford, F.; Yuzawa, T.; Platz, M. S.; Matzinger, S.; Fulscher, M. J. *Am. Chem. Soc.* **1998**, *120*, 4430.
- (53) Moss, R. A.; Yan, S.; Krogh-Jespersen, K. *J. Am. Chem. Soc.* **1998**, *120*, 1088.
- (54) Merrer, D. C.; Moss, R. A.; Liu, M. T. H.; Banks, J. T.; Ingold, K. U. *J. Org. Chem.* **1998**, *63*, 3010.
- (55) Pezacki, J. P.; Warkentin, J.; Wood, P. D.; Luszytk, J.; Yuzawa, T.; Gudmundsdottir, A. D.; Morgan, S.; Platz, M. S. *J. Photochem. Photobiol. A* **1998**, *116*, 1.
- (56) Bonneau, R.; Hellrung, B.; Liu, M. T. H.; Wirz, J. *J. Photochem. Photobiol. A* **1998**, *116*, 9.
- (57) Bonneau, R.; Liu, M. T. H. *Adv. Carbene Chem.* **1998**, *2*, 1.
- (58) Tae, E. L.; Zhu, Z.; Platz, M. S.; Pezacki, J. P.; Warkentin, J. *J. Phys. Chem. A* **1999**, *103*, 5336.
- (59) Pezacki, J. P.; Couture, P.; Dunn, J. A.; Warkentin, J.; Wood, P. D.; Luszytk, J.; Ford, F.; Platz, M. S. *J. Org. Chem.* **1999**, *64*, 4456.
- (60) Evansck, J. D.; Houk, K. N. *J. Phys. Chem.* **1990**, *94*, 5518.
- (61) Evansck, J. D.; Houk, K. N. *J. Am. Chem. Soc.* **1990**, *112*, 9148.
- (62) Storer, J. W.; Houk, K. N. *J. Am. Chem. Soc.* **1993**, *115*, 10426.
- (63) Yamamoto, N.; Bernardi, F.; Bottoni, A.; Olivucci, M.; Robb, M. A.; Wilsey, S. *J. Am. Chem. Soc.* **1994**, *116*, 2064.
- (64) Cramer, C. J.; Truhlar, D. G.; Falvey, D. E. *J. Am. Chem. Soc.* **1997**, *119*, 12338.
- (65) Keating, A. E.; Garcia-Garibay, M. A.; Houk, K. N. *J. Am. Chem. Soc.* **1997**, *119*, 10805.
- (66) Sulzbach, H. M.; Platz, M. S.; Schaefer, H. F.; Hadad, C. M. *J. Am. Chem. Soc.* **1997**, *119*, 5682.
- (67) Shustov, G. V.; Liu, M. T. H.; Rauk, A. *J. Phys. Chem. A* **1997**, *101*, 2509.
- (68) Patterson, E. V.; McMahon, R. J. *J. Org. Chem.* **1997**, *62*, 4398.
- (69) Keating, A. E.; Garcia-Garibay, M. A.; Houk, K. N. *J. Phys. Chem. A* **1998**, *102*, 8467.
- (70) Shustov, G. V.; Liu, M. T. H.; Houk, K. N. *Can. J. Chem.* **1999**, *77*, 540.
- (71) Garrett, B. C.; Truhlar, D. G. *J. Chem. Phys.* **1979**, *70*, 1593.
- (72) Garrett, B. C.; Truhlar, D. G. *J. Chem. Phys.* **1984**, *81*, 309.
- (73) Truhlar, D. G.; Garrett, B. C.; Hipes, P. G.; Kuppermann, A. *J. Chem. Phys.* **1984**, *81*, 3542.
- (74) Truhlar, D. G.; Isaacson, A. D.; Garrett, B. C. In *Theory of Chemical Reaction Dynamics*; Baer, M., Ed.; CRC Press: Boca Raton, FL, 1985; Vol. 4, p 65.
- (75) Kreevoy, M. M.; Truhlar, D. G. In *Investigation of Rates and Mechanisms of Reactions*; Bernasconi, C. F., Ed.; Techniques of Chemistry Series 6; John Wiley & Sons: New York, 1986; Part 1, p 13.
- (76) Tucker, S. C.; Truhlar, D. G. In *New Theoretical Concepts for Understanding Organic Reactions*; Bertran, J. I. G. C., Ed.; NATO ASI Series C267; Kluwer Academic Publishers: Dordrecht, 1989; p 291.
- (77) Truhlar, D. G.; Garrett, B. C.; Klippenstein, S. J. *J. Phys. Chem.* **1996**, *100*, 12771.
- (78) Lu, D.-h.; Truong, T. N.; Melissas, V. S.; Lynch, G. C.; Liu, Y.-P.; Garrett, B. C.; Steckler, R.; Isaacson, A. D.; Rai, S. N.; Hancock, G. C.; Lauderdale, J. G.; Joseph, T.; Truhlar, D. G. *Comput. Phys. Commun.* **1992**, *71*, 235.
- (79) Liu, Y. P.; Lynch, G. C.; Truong, T. N.; Lu, D. H.; Truhlar, D. G.; Garrett, B. C. *J. Am. Chem. Soc.* **1993**, *115*, 2408.
- (80) Corchado, J. C.; Chuang, Y.-Y.; Coitiño, E. L.; Truhlar, D. G. GAUSSRATE-version 8.6; University of Minnesota, Minneapolis, 2000.
- (81) Corchado, J. C.; Chuang, Y.-Y.; Fast, P. L.; Villá, J.; Hu, W.-P.; Liu, Y.-P.; Lynch, G. C.; Nguyen, K. A.; Jakels, C. F.; Melissas, V. S.; Lynch, B. J.; Rossi, I.; Coitiño, E. L.; Fernandez-Ramos, A.; Steckler, R.; Garrett, B. C.; Isaacson, A. D.; Truhlar, D. G. POLYRATE-version 8.5.1; University of Minnesota, Minneapolis, 2000.
- (82) Frisch, M. J.; Trucks, G. W.; Schlegel, H. B.; Scuseria, G. E.; Robb, M. A.; Cheeseman, J. R.; Zakrzewski, V. G.; Montgomery, J. A.; Stratmann, R. E.; Burant, J. C.; Dapprich, S.; Millam, J. M.; Daniels, A. D.; Kudin, K. N.; Strain, M. C.; Farkas, O.; Tomasi, J.; Barone, V.; Cossi, M.; Cammi, R.; Mennucci, B.; Pomelli, C.; Adamo, C.; Clifford, S.; Ochterski, J.; Petersson, G. A.; Ayala, P. Y.; Cui, Q.; Morokuma, K.; Malick, D. K.; Rabuck, A. D.; Raghavachari, K.; Foresman, J. B.; Cioslowski, J.; Ortiz, J. V.; Stefanov, B. B.; Liu, G.; Liashenko, A.; Piskorz, P.; Komaromi, I.; Gomperts, R.; Martin, R. L.; Fox, D. J.; Keith, T.; Al-Laham, M. A.; Peng, C. Y.; Nanayakkara, A.; Gonzalez, C.; Challacombe, M.; Gill, P. M. W.; Johnson, B. G.; Chen, W.; Wong, M. W.; Andres, J. L.; Head-Gordon, M.; Replogle, E. S.; Pople, J. A. *Gaussian 98* (Revision A.9); Pittsburgh, PA, 1998.
- (83) Page, M.; McIver, J. W., Jr. *J. Chem. Phys.* **1988**, *88*, 922.
- (84) Chuang, Y.-Y.; Truhlar, D. G. *J. Phys. Chem. A* **1998**, *102*, 242.
- (85) Hehre, W. J.; Radom, L.; Schleyer, P. R.; Pople, J. A. *Ab Initio Molecular Orbital Theory*; Wiley: New York, 1986.
- (86) Lynch, B. J.; Fast, P. L.; Harris, M.; Truhlar, D. G. *J. Phys. Chem. A* **2000**, *104*, 4811.
- (87) Adamo, C.; Barone, V. *J. Chem. Phys.* **1998**, *108*, 664.
- (88) Lee, C.; Yang, W.; Parr, R. G. *Phys. Rev. B* **1988**, *37*, 785.
- (89) Becke, A. D. *J. Chem. Phys.* **1993**, *98*, 5648.

- (90) Stephens, P. J.; Devlin, F. J.; Chabalowski, C. F.; Frisch, M. J. *J. Phys. Chem.* **1994**, *98*, 11623.
- (91) Ochterski, J. W.; Petersson, G. A.; Montgomery, J. A., Jr. *J. Chem. Phys.* **1996**, *104*, 2598.
- (92) Fast, P. L.; Truhlar, D. G. *J. Phys. Chem. A* **2000**, *104*, 6111.
- (93) Rodgers, J. M.; Fast, P. L.; Truhlar, D. G. *J. Chem. Phys.* **2000**, *112*, 3141.
- (94) Fast, P. L.; Sanchez, M. L.; Truhlar, D. G. *Chem. Phys. Lett.* **1999**, *306*, 407.
- (95) Tratz, C. M.; Fast, P. L.; Truhlar, D. G. *Phys. Chem. Commun.* **1999**, *2*, Article 14.
- (96) Fast, P. L.; Corchado, J. C.; Sanchez, M. L.; Truhlar, D. G. *J. Phys. Chem. A* **1999**, *103*, 5129.
- (97) Roos, B. *Adv. Chem. Phys.* **1987**, *69*, 399.
- (98) Andersson, K.; Malmqvist, P. A.; Roos, B. O. *J. Chem. Phys.* **1992**, *96*, 1218.
- (99) Dunning, T. H., Jr. *J. Chem. Phys.* **1989**, *90*, 1007.
- (100) Andersson, K.; Blomberg, M. R. A.; Fulscher, M. P.; Karlstroem, G.; Lindh, R.; Malmqvist, P. A.; Neogrady, P.; Olsen, J.; Roos, B. O.; Sadlej, A. J.; Schutz, M.; Seijo, L.; Serrano-Andres, L.; Siegbahn, P. E. M.; Widmark, P. O. MOLCAS-version 4; Lund University, Lund, Sweden, 1997.
- (101) Rodgers, J. M.; Lynch, B. J.; Fast, P. L.; Chuang, Y.-Y.; Pu, J.; Truhlar, D. G. MULTILEVEL-version 2.3; University of Minnesota, Minneapolis, 2001.
- (102) Xidos, J. D.; Li, J.; Hawkins, G. D.; Winget, P. D.; Zhu, T.; Rinaldi, D.; Liotard, D. A.; Cramer, C. J.; Truhlar, D. G.; Frisch, M. J. MN-GSM-version 99.8; University of Minnesota, Minneapolis, 2001.
- (103) Hoijsink, G. J.; de Boer, E.; van der Meij, P. H.; Weijland, W. P. *Rec. Trav. Chim. Pays-Bas* **1956**, *75*, 487.
- (104) Chalvet, O.; Jano, I. *Compt. Rend.* **1964**, *259*, 1867.
- (105) Jano, I. *Compt. Rend.* **1965**, *261*, 103.
- (106) Constanciel, R.; Tapia, O. *Theor. Chim. Acta* **1978**, *48*, 75.
- (107) Tapia, O.; Silvi, B. J. *Phys. Chem.* **1980**, *84*, 2646.
- (108) Constanciel, R.; Contreras, R. *Theor. Chim. Acta* **1984**, *65*, 1.
- (109) Contreras, R.; Aizman, A. *Int. J. Quantum Chem.* **1985**, *27*, 293.
- (110) Tucker, S. C.; Truhlar, D. G. *Chem. Phys. Lett.* **1989**, *157*, 164.
- (111) Kozaki, T.; Morihashi, K.; Kikuchi, O. *J. Am. Chem. Soc.* **1989**, *111*, 1547.
- (112) Still, W. C.; Tempczyk, A.; Hawley, R. C.; Hendrickson, T. J. *Am. Chem. Soc.* **1990**, *112*, 6127.
- (113) Cramer, C. J.; Truhlar, D. G. In *Quantitative Treatments of Solute/Solvent Interactions*; Politzer, P., Murray, J. S., Eds.; Theoretical and Computational Chemistry Series 1; Elsevier: Amsterdam, 1994; p 9.
- (114) Cramer, C. J.; Truhlar, D. G. *Chem. Rev.* **1999**, *99*, 2161.
- (115) Zhu, T.; Li, J.; Hawkins, G. D.; Cramer, C. J.; Truhlar, D. G. *J. Chem. Phys.* **1998**, *109*, 9117.
- (116) Hawkins, G. D.; Zhu, T.; Li, J.; Chambers, C. C.; Giesen, D. J.; Liotard, D. A.; Cramer, C. J.; Truhlar, D. G. In *Combined Quantum Mechanical and Molecular Mechanical Methods*; Gao, J., Thompson, M. A., Eds.; ACS Symposium Series 712; American Chemical Society: Washington, DC, 1998; p 201.
- (117) Li, J.; Zhu, T.; Hawkins, G. D.; Winget, P.; Liotard, D. A.; Cramer, C. J.; Truhlar, D. G. *Theor. Chem. Acc.* **1999**, *103*, 9.
- (118) Lowdin, P. O. *J. Chem. Phys.* **1950**, *18*, 365.
- (119) Li, J.; Zhu, T.; Cramer, C. J.; Truhlar, D. G. *J. Phys. Chem. A* **1998**, *102*, 1820.
- (120) Zhu, T.; Li, J.; Liotard, D. A.; Cramer, C. J.; Truhlar, D. G. *J. Chem. Phys.* **1999**, *110*, 5503.
- (121) Chuang, Y.-Y.; Cramer, C. J.; Truhlar, D. G. *Int. J. Quantum Chem.* **1998**, *70*, 887.
- (122) Chuang, Y.-Y.; Radhakrishnan, M. L.; Fast, P. L.; Cramer, C. J.; Truhlar, D. G. *J. Phys. Chem. A* **1999**, *103*, 4893.
- (123) Chuang, Y.-Y.; Corchado, J. C.; Truhlar, D. G. *J. Phys. Chem. A* **1999**, *103*, 1140.
- (124) Truhlar, D. G.; Lu, D. H.; Tucker, S. C.; Zhao, X. G.; Gonzalez-Lafont, A.; Truong, T. N.; Maurice, D.; Liu, Y. P.; Lynch, G. C. In *Isotope Effects in Gas-Phase Chemistry*; ACS Symposium Series 502; American Chemical Society: Washington, DC, 1992; p 16.
- (125) Truong, T. N.; Lu, D.-h.; Lynch, G. C.; Liu, Y.-P.; Melissas, V. S.; Stewart, J. J. P.; Steckler, R.; Garrett, B. C.; Isaacson, A. D.; Gonzalez-Lafont, A.; Rai, S. N.; Hancock, G. C.; Joseph, T.; Truhlar, D. G. *Comput. Phys. Commun.* **1993**, *75*, 143.
- (126) Fernandez-Ramos, A.; Truhlar, D. G. *J. Chem. Phys.* **2001**, *114*, 1491.
- (127) Bridge, M. R.; Frey, H. M.; Liu, M. T. H. *J. Chem. Soc. A* **1969**, 91.
- (128) Archer, W. H.; Tyler, B. J. *J. Chem. Soc., Faraday Trans. 1* **1976**, *72*, 1448.
- (129) Frey, H. M.; Penny, D. E. *J. Chem. Soc., Faraday Trans. 1* **1977**, *73*, 2010.
- (130) Figuera, J. M.; Tobar, A. *J. Photochem.* **1979**, *10*, 473.
- (131) Becerra, R.; Figuera, J. M.; Martinez Utrilla, R.; Castillejo, M.; Menendez, V. *An. Quim., Ser. A* **1984**, *80*, 502.
- (132) Avila, M. J.; Becerra, R.; Figuera, J. M.; Rodriguez, J. C.; Tobar, A.; Martinez-Utrilla, R. *J. Phys. Chem.* **1985**, *89*, 5489.
- (133) Alhambra, C.; Gao, J. L.; Corchado, J. C.; Villa, J.; Truhlar, D. G. *J. Am. Chem. Soc.* **1999**, *121*, 2253.
- (134) Truong, T. N.; McCammon, J. A. *J. Am. Chem. Soc.* **1991**, *113*, 7504.
- (135) Corchado, J. C.; Espinosa-Garcia, J. *J. Chem. Phys.* **1996**, *105*, 3160.
- (136) Villa, J.; Gonzalez-Lafont, A.; Lluch, J. M. *J. Phys. Chem.* **1996**, *100*, 19389.
- (137) Hu, W.-P.; Rossi, I.; Corchado, J. C.; Truhlar, D. G. *J. Phys. Chem. A* **1997**, *101*, 6911.
- (138) Storer, J. W. Private communication.
- (139) Riehl, J. F.; Morokuma, K. *J. Chem. Phys.* **1994**, *100*, 8976.
- (140) It is interesting that, as shown in Table 7, the CBS-Q and MCCC results are very close to MPW1KH DFT result. The fact that mPW1PW91 apparently underestimates the barrier for reaction R-1 is not entirely surprising.⁸⁶ This finding gives us some confidence that mPW1PW91 does not seriously overestimate the barrier heights for reactions R-2, R-3, and R-4.
- (141) We also investigated the reaction in the gas phase using MPW1K/6-31+G(d,p) theory and found similar results. In particular, when using the MPW1K functional, the calculated $k^{V/T}$ rate constants are about four times smaller than the mPW1PW91/6-31+G(d,p) ones for **5a** \rightarrow **7a** (as a result of a 0.9 kcal/mol higher barrier height) and about five times smaller for **5a** \rightarrow **6a** (as a result of a 1.0 kcal/mol higher barrier height).
- (142) Albu, T. V.; Corchado, J. C.; Truhlar, D. G. *J. Phys. Chem. A* **2001**, *105*, 8465.
- (143) Pauling, L. *The Nature of the Chemical Bond and the Structure of Molecules and Crystals. An Introduction to Modern Structural Chemistry*, 3rd ed.; Cornell University Press: Ithaca, NY, 1960.
- (144) Mayer, I. *Chem. Phys. Lett.* **1983**, *97*, 270.
- (145) Hayes, R. L.; Fattal, E.; Govind, N.; Carter, E. A. *J. Am. Chem. Soc.* **2001**, *123*, 641.
- (146) Scott, A. P.; Platz, M. S.; Radom, L. *J. Am. Chem. Soc.* **2001**, *123*, 6069.
- (147) Krogh-Jespersen, K.; Yan, S.; Moss, R. A. *J. Am. Chem. Soc.* **1999**, *121*, 6269.